Fabrication and Evaluation of Perovskite $LaCrO_3$ Nanoparticles as Catalyst for Electrochemical Ammonia Synthesis

Mathilda Ohrelius

Thesis for the degree of Master of Science in Engineering
Division of Heat Transfer
Department of Energy Sciences
Faculty of Engineering | Lund University

Fabrication and Evaluation of Perovskite $LaCrO_3$ Nanoparticles as Catalyst for Electrochemical Ammonia Synthesis

Mathilda Ohrelius

May 2019, Lund

This degree project for the degree of Master of Science in Engineering has been conducted at the Division of Heat Transfer, Department of Energy Sciences, Faculty of Engineering, Lund University, and at the School of Materials and Energy, University of Electronic Science and Technology of China

Supervisor at the Division of Heat Transfer was Dr Martin Andersson
Supervisor at University of Electronic Science and Technology of China was Dr Ting Shuai Li
Examiner at Lund University was Dr Lei Wang

Thesis for the Degree of Master of Science in Engineering

ISRN LUTMDN/TMHP-19/5434-SE

ISSN 0282-1990

Division of Heat Transfer
Department of Energy Sciences
Faculty of Engineering, Lund University
Box 118, 221 00 Lund
Sweden

www.energy.lth.se

Abstract

As our way of living exploits the resources of the earth and our energy use keeps on increasing, we are now facing a climate crisis never seen before in modern time. To face these consequences and try to ease the harm we need to transform our extraction and use of energy. The use of chemical energy carriers and fuel cells offers the possibility of a completely green solution for energy distribution and conversion. A fuel cell converts chemical energy into electrical energy through a series of chemical and electrochemical reactions. Hydrogen has been the dominating fuel for fuel cells but a large obstacle for commercialization is the distribution infrastructure that needs to be planted. This problem has opened the way for another chemical energy carrier with a widely developed infrastructure. Ammonia (NH_3) is one of the most produced chemical substances globally, mainly used for fertilizers. It's easier to store and transport than hydrogen but the big challenge is the industrial ammonia synthesis, a heavily energy consuming process.

This Master's thesis focus on the production of an active and selective catalyst for the electrochemical ammonia synthesis. A primary study was performed to investigate previous reported results of catalyst designs for the nitrogen reduction reaction (NRR). Noble metals have been proved to be stable and active catalysts but to decrease the cost of the material, transition metals offers a great alternative. To reach the performance as for the traditional Haber-Bosch process the catalyst need to be optimized. One approach to this is a nanoscale design of the catalyst to improve the availability of the active sites and the mass transfer. The perovskite $LaCrO_3$ is a ceramic material with great properties for heterogenous catalysis. The perovskite material is thermally stable with a great flexibility in tailoring the structure down to atom level. The highest ammonia yield was obtained at -0.8 V vs. RHE with an ammonia formation rate of 24.8 $\mu g\ h^{-1}\ mg^{-1}_{cat}$, and a Faradic efficiency of 15%. The results offer a great alternative with the easily produced and low-cost perovskite structured electrocatalysts for NRR.

To find the perfect NRR electrocatalyst experimental and theoretical work needs to be furthered improved. One important aspect of this work is to get detailed material characterizations to investigate structure, particle size, surface properties, and electrical conductivity of the catalysts. From this, a relation between the catalytic activity and solid-state properties can be drawn and further material design strategies can be conducted. A detailed characterization of the as-produced $LaCrO_3$ crystals are therefore also conducted in the experimental part of this thesis, together with the electrochemical ammonia synthesis testing.

Keywords: nitrogen reduction reaction, electrochemical ammonia synthesis, catalyst, perovskite, LaCrO3, fuel cell, renewable energy

List of publications

This thesis is based on the following paper:

- M. Ohrelius, Y. Li, H. Xian, G. Yu, Q. Wang, T. Li, M. Andersson "Electrochemical Synthesis of Ammonia Based on Perovskite $LaCrO_3$ Catalyst", (to be submitted to journal)

Preface

This master thesis was performed at University of Electronic Science and Technology of China (UESTC) as a collaboration between the department of Energy Sciences at Lund University and the department of Materials and Energy at UESTC. The thesis is a 30 ECTS project, which is full time of one semester. The experiments were conducted during 15 weeks in Chengdu, China, with the purpose of performing research on ammonia synthesis as well as experiencing a foreign culture.

The financial support for the project was generously provided from ÅForsk travel grant and Fredrika Bremer Förbundets Stipendiestiftelse. I would like to acknowledge my supervisors Dr. Martin Andersson and Dr. Ting Shuai Li for the support and encouragement during the research. A special thanks to Guangsen Yu, Haohong Xian and Yuanfang Li, my lab partners who have provided guidance and help during the project. A final thanks to the Chinese students of UESTC and Dr. Li for generously welcoming me into their group and giving me an unforgettable time in China.

Mathilda Ohrelius
Lund, May 2019

Contents

List of Figures

List of Tables

Introduction

It is well known that the way we live our lives today have a striking effecting on the climate and the nature around us. That the natural resources we are consuming is way above the limit to keep a balance in the ecosystem on earth. In the modern world our energy use has constantly increased since the beginning of industrialization. Our living conditions have gotten more energy demanding together with a growing population on earth (1).

Since pre-industrial time the average temperature on earth has risen 1.0°C because of human impact according to the IPCC Special Report "Global Warming of 1.5°C". The global warming caused by emissions of greenhouse gases have devastating consequences on the nature both in our near environment as well as far away from our cities. One acute threat is the air pollution in the rapidly growing cities with the burning of fossil fuels for heat and transportation. China being one example where in many of the big cities the SO_2, NO_x and PM emissions are exceeding the World Health Organization's air quality standards. According to WHO 2.2 million of the world's premature deaths annually from indoor and ambient air pollution are in the Asia Pacific region (2).

To reduce our dependence on fossil fuels, introducing more renewable energy sources will be crucial to turn the trend of global warming and air pollution. Together with a decrease of our CO_2 emissions one of the technical challenges is how to take care of the energy we produce in the most efficient way. This covers the conversion process of for example wind energy to electricity, as well as the storing and transportation of the energy carrier. To have large-scale economical storage capability for energy is also a key technology for the energy revolution. The pressure on the power grid and the irregularity caused by the introduction of renewable energy sources have a significant effect on both the performance and reliability on our electricity supply (3).

Fuel cells are similar to batteries in their way of chemically converting energy directly into electricity but with the advantage that they are continuously operating, as long as fueled. They are cleaner and more efficient than the traditional combustion engines where a lot of the chemical energy is released in the exhaust gases. When fuelled with hydrogen, the only by-product from the fuel cell is water which makes them a great alternative for electrical energy conversion. For fuel cells to be able to replace the traditional combustion engines they need to become more economical and efficient in a large scale (4).

Hydrogen together with natural gas are the dominating fuels for fuel cells today, but recently ammonia has risen as an alternative. Ammonia as an energy carrier has advantages when it comes to its chemical properties but mainly because of the already existing infrastructure in the world. Ammonia synthesis or NRR (nitrogen reduction reaction), is an industrial process that have a great impact on our lives today. Since ammonia is the main component in fertilisers, this process, developed in 1913 played a big part in enabling the population growth

on the planet. The main challenge with today's industrial ammonia production is the great energy consumption it needs when produced through the Haber-Bosch process. As well as the main feedstock coming from natural gas, releasing a great amount of CO_2.

A great amount of research has during the last decades been done to find new ways for ammonia synthesis under less harsh conditions. The electrochemical NRR has the advantage that it can give an overpotential to the process produced by renewable energy sources (5). The catalyst plays an essential role for the cost and efficiency of the NRR. Noble metals have played an important role in catalysis because of their advantageous properties. The disadvantage is their high prize and accessibility and to replace the noble metal catalyst systems with high-performance and inexpensive electrocatalysts is critical for large-scale industrial applications (6).

Low cost and earth abundance make transition metals a great alternative to replace noble metal catalysts (7). Together with the fast development in the science of nanomaterials, a new approach to catalyst design has emerged. The ability to keep precise control over size and composition of the material, further with the possibility to assemble them into large structures has been showed to offer great potentials. It has been discovered that these materials, usually in the scale of 1-100nm gain unique sets of properties comparing with the traditionally used industrial materials today (8). If combining transition metals with metal oxides (increasing the stability), a perovskite structured material (ABO_3) can be synthesised. This offers great characteristics for a catalyst, with a flexible, crystalline structured and thermally stable material (9).

To find the perfect NRR electrocatalyst experimental and theoretical work needs to be furthered conducted. One important aspect of this is to get detailed material characterizations to investigate structure, particle size, surface properties, and electrical conductivity of the as-prepared catalysts. From this, a relation between the catalytic activity and solid-state properties can be developed as well as new material design strategies.

1 Aim

The aim of this study was to synthesize perovskite $LaCrO_3$ nanoparticles and characterize and evaluate as a potential catalyst for the electrochemical nitrogen reduction reaction. Previous transition metal and transition metal oxides have been tested by others, but the perovskite nanostructure is a new approach in the field of NRR. In order to evaluate the activity for NRR, electrochemical testing was performed in a H-type cell. A vast characterization of the prepared material was also conducted with several spectroscopic methods. This to evaluate the material properties and its performance and to contribute with key data for the future development of an optimized NRR catalyst.

The following research questions were to be answered:

- Can hydrothermally synthesized $LaCrO_3$ act as an active and selective catalyst for electrochemical NRR?
- What characteristics will the hydrothermally synthesized $LaCrO_3$ obtain?
- What characteristics are preferred for the optimized electrocatalyst?

2 Limitations

The major part of the Master's thesis was performed at University of Electronic Science and Technology of China (UESTC). This because of a cooperation between the department of Energy Sciences at Lund University and the department of materials and energy on UESTC, that performs experimental research in addition to Lund University's theoretical orientation.

Due to a limited amount of time the hydrothermal synthesis for $LaCrO_3$ could not be fully explored to find the optimal reaction parameters. Only one way of heat treatment was performed, chosen and inspired from other paper's results. The furnace accessible had limited heating intervals and programs and a better result could have been obtained if the heating intervals would have been explored with several material preparations.

The equipment was shared with other students so the access to the lab equipment was sometimes restricted. The SEM pictures were received from Sichuan University, since the equipment needed was unavailable at UESTC.

3 Outline

The thesis is divided into 6 chapters and 2 appendices with the following content:

- **Chapter 2 "Ammonia for Power"** describes the fundamentals of SOFCs and the role of chemical energy carriers. The history of ammonia synthesis is described and the biological synthesis as well as industrial ways to produce ammonia. Furthermore, the role of the catalyst is explained and different methods to design an efficient electrocatalyst.
- **Chapter 3 "Methodology"** is divided into two parts; firstly, a short description of the hydrothermal synthesis method, electrochemical testing and material characterization methods, and secondly, the specific setup used and how the experiments were conducted.
- **Chapter 4 "Results"** presents the results of the performed experiments.
- **Chapter 5 "Discussion"** carries the discussion of the results and describes the potential sources of errors.
- **Chapter 6 "Conclusion and Further Research"** presents the conclusions of the performed research and suggestions of further studies to complete the analysis.
- **Appendix A** shows a comparison table of other experimental research result of electrocatalysts for NRR
- **Appendix B** shows the remaining SEM and TEM pictures not included in the results.

1 Fuel Cell Technology

Fuel cells are similar to batteries in their way of chemically converting energy directly into electricity but with the advantage that they are continuously operating, as long as fueled. They are fueled with hydrogen-rich gas from commonly available fuels such as gasoline or natural gas, together with an oxidant, such as air. The big advantage is that when fueled with pure hydrogen and oxygen as oxidant, the only byproduct is water (10).

The basic building block of a fuel cell consists of a porous anode and cathode separated by an electrolyte layer, see Figure 1 (4). In the dual chamber fuel cell, a fuel enters the anode and an oxidant enters the cathode. These are separated by a selectively conductive electrolyte were the conduction can occur in either direction depending on the fuel cell. The fuel cell can be designed so that specific species will conduct, called charge carriers, such as H^+, CO_3^{2-}, O^{2-} etc. When designed in this way the fuel or oxidant must be transformed in the electrodes into that specific charge carrier. The different types of fuel cells are besides type of charge carrier categorized on the type of electrolyte used in the cells and the operating temperature (4).

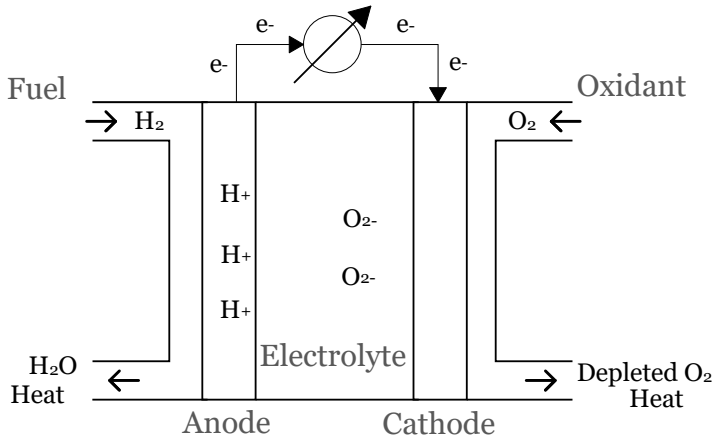

Figure 1: Basic model of a fuel cell fuelled by hydrogen gas

Low temperature operating fuel cells like alkaline and polymer membrane (PEM) fuel cells are beneficial in their fast start up time and favorable power-to-weight ratio. This makes them appropriate to use in vehicles and mobile generators. The low temperature condition puts higher requirements on the catalyst to be active than for the high temperature cells where the reaction rate is automatically higher. The best catalyst, but also the most expensive ones require noble metals and H_2 is then the only acceptable fuel for the catalyst to resist poisoning (11). In high-temperature fuel cells like solid oxide (SOFC) and molten carbonate fuel cell, less expensive catalysts can be used. Other types of fuels can also be used such as CO and CH_4 since the catalysts are less sensitive

to poisoning. High temperature fuel cells can for example be used in small- and big-scale stationary power applications (4).

In the standard fuel cell electrical energy is generated by the exothermic oxidation of hydrogen, where electrons are removed from H_2, see Equation 1. The aim of a fuel cell is to achieve full oxidation of its fuel to extract the maximum thermodynamic output. This requires efficient catalysts, to keep the reaction temperature low and still have a satisfying reaction rate (4).

$$H_2 - 2e^- \rightarrow 2H^+ \quad (1)$$

2 Electrochemistry

The science of electrochemistry is about the interconversion between energy in chemical and electric form. It can result in the direct production of electricity from a raw material and for electrolytic processes, the production of chemical products and metals. This field of science is growing as batteries and fuel cells are taking a bigger role in our energy utilization. For fuel cell technology electrochemistry plays an important role in two aspects. Firstly, to understand and optimize the processes occurring in the fuel cell itself. But also, to use for investigation and characterization of candidate catalysts materials for use in the cell. Electrochemical techniques can test and quantify the activity for many of the catalysts and solid-state devices. Another interesting aspect is the development of new materials, where properties associated with electron transfer are getting more and more attention. For issues related to energy technology, electronics, environment and health care nanomaterials offers a new type of solutions where the fields of nanoscience and electrochemistry are closely associated (12). One great example is electrochemical storage where the challenging reactions to convert stored energy into power (particularly multielectron reactions) now can be performed reversible and kinetically facile. This by changing the reaction pathway by introducing doped nanoscale electrode materials (13).

Furthermore, electrochemical reactions are the most efficient ways to convert chemical energy into electrical. Chemical energy can be generated from the sun and stored in the form of coal, petroleum or biomass for example. With an electrochemical reaction an ideal efficiency of close to 100% electrical energy output from the fuel is possible. This is a great advantage over the traditional combustion engines where a lot of chemical energy is released in the exhaust gases. In the electrochemical cell the reactions are carried out with the result of an overpotential. If current is allowed to flow the electrochemical overpotential can result in a charge transfer (4). The reverse reaction is electrolysis, the process for charging a battery. Then an external electrical source is connected and supplies energy to the system for a non-spontaneous reaction to occur.

The applied voltage offers an additional degree of freedom to the electrochemical system. This makes electrosynthesis a popular method in the industry for material production. Compared to the thermal synthesis process for material production, the higher energetic yield is the other advantage. This offers the possibility to vary the energy of the active species and to attain a high selective reactivity even in low temperatures (14).

A major topic in the field of electrochemistry is the knowledge about the interfaces between materials. The matters in the fuel cell, the fuel and the oxidant, are transformed via electron shifts at the atomic level. The transformations are called oxidation-reduction reactions, or redox reaction. When a chemical element loses one or more electrons it undergoes an oxidation. When electrons are gained, it's instead called to undergo a reduction. These two phenomena are called half-reactions and the resulting redox reaction is Equation 2 (14). An electrochemical setup for studying a system working as a power source is demonstrated in Figure 2

$$\mathrm{Red} \underset{reduction}{\overset{oxidation}{\rightleftharpoons}} = \mathrm{Ox} + ne^{-} \tag{2}$$

Some of the species involved in the fuel cell reactions are ionic. The anion has a negative sign, the same as that of the electron, and the cation has a positive sign. Although, there is no link between the charge of the ion and its oxidizing or reducing properties (14).

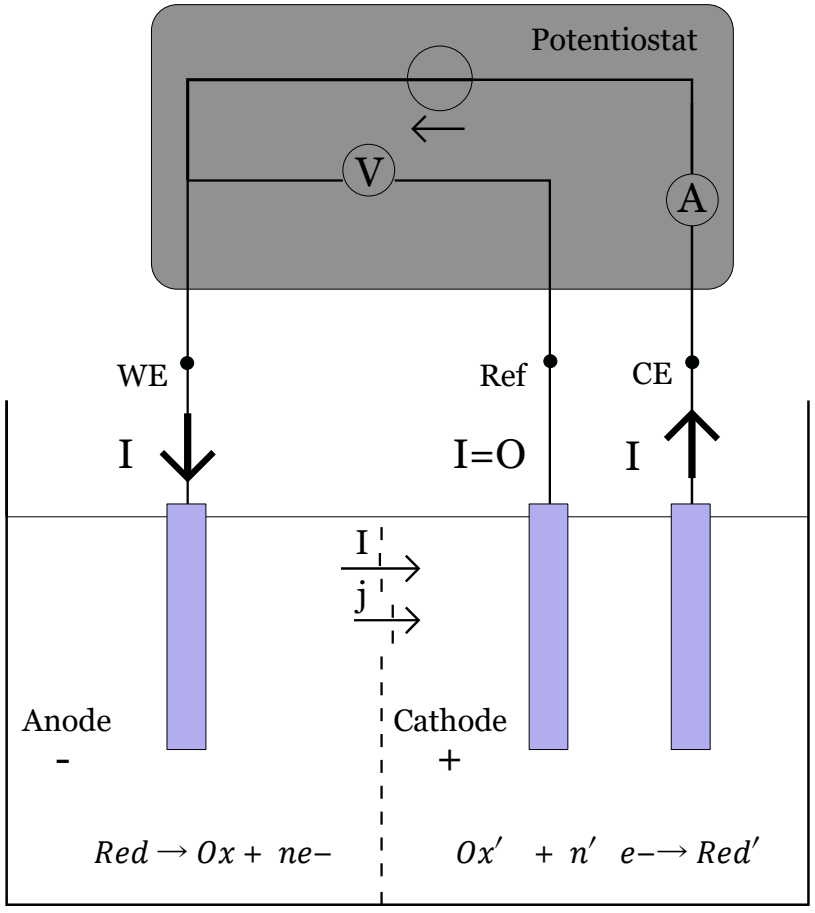

Figure 2: Simplified diagram of an electrochemical setup using a potentiostat with inspiration from (14). WE: working electrode; Ref: reference electrode; CE: counter electrode

3 Chemical Energy Carriers

In the search for a fuel that doesn't require the burning of fossil fuels, chemical energy carriers offer great possibilities. The purpose of an energy carrier is to

store and convert energy without any losses. The energy created from renewable sources can be stored in this way and then used later at a time and place where the energy is needed. The right energy carrier will improve the quality in the whole supply chain from primary source to final application. When comparing various storage technologies such as thermo-mechanical storage, pumped hydro, batteries, chemicals and super capacitors, chemical storage can cover very large energy capacities and it also offers a broad power range. Compared to the more commercial Li-ion batteries, chemical energy carriers have the possibility to store larger quantities of energy over longer periods of time (5).

3.1 Hydrogen

Hydrogen is the most studied energy carrier for fuel cells. As a fuel vector it's a simple and abundant element, high in energy and leaving no pollution when reacting in the fuel cell. It has been dominating the literature as the superior fuel, running with very high efficiency in PEM fuel cells (11). However, H_2 is today mainly manufactured from natural gas through the steam reforming of methane. This process uses a high energy density fuel and water to produce hydrogen and carbon monoxide (15). The production can also be made from H_2O and powered by renewable energy sources. In this way the whole process can be performed completely emission free (16).

To become commercial the hydrogen storage method must offer high volumetric storage capacity and gravimetric density, as well as fast kinetics of hydrogen charge/discharge. One major disadvantage of the hydrogen is its properties for storing and the need for large volumes when carried in molecular form. The hydrogen commercially available today requires very high pressures to approach to target for volumetric density. In the industry hydrogen is usually compressed at 20-25MPa and stored in stainless steel bottles. This results in a high cost for the pressurization as well as a the large pressure drop inside the tank during use (17). The other great challenge is the hydrogen refueling infrastructure. This would have to be widely built and maintained to make hydrogen fuel a possible replacement for gasoline (13).

3.2 Ammonia

As the second most produced chemical substance globally and with its high hydrogen content ammonia (NH_3) has a great potential as a promising fuel for fuel cells (18). In 2017 a total of 150 million tons of ammonia was manufactured in the world (19). Except for being used in fertilisers (88%), ammonia is used in explosives, pharmaceuticals, cleaning products and many other industrial processes (20). It is widely distributed with an established market and a transport and storage infrastructure (5). Because of that, ammonia has in recent years started to gain attention for its possibility as a future green energy carrier (20).

Ammonia is an alkaline, colorless and lighter than air gas with a penetrating odor (21). Like synthesized hydrogen, ammonia is a product that can be obtained either from geological sources or biological. From processes powered by renewable sources such as wind and photovoltaics the entire N_2/NH_3 cycle

can be made completely carbon free (5). Ammonia can then be used either directly in the high temperature fuel cells or converted to H_2 before use (22).

One mol of ammonia contains 1.5 mol of hydrogen which is 17.8% by weight. This gives 108 kg H_2/m_3 embedded in liquid ammonia at 20˚C and 8.6 bars (23). The high gravimetric hydrogen content is a great advantage for the application in fuel cells. The volumetric energy of ammonia 10.4-13.6 GJ/m^3, is higher compared to hydrogen 3.6GJ/m^3 (24). Ammonia is also easier to transport, and store and the volumetric density of liquefied ammonia is higher than that of liquefied hydrogen. The boiling point for liquefied ammonia is -33 ˚C at atmospheric pressure and it stays in liquid form above about 9-10 bar pressure at ambient temperature (15). When looking at the costs its therefore cheaper in per unit of stored energy with ammonia 0.54$/kg-$H_2$ than pure hydrogen storage 14.95$/kg-$H_2$ (22).

4 Solid Oxide Fuel Cell

The SOFC is an oxygen ion conductor and the electrolyte is therefor designed to only let oxygen ions pass. Oxygen is fed to the cathode side and reduced under a catalyst into O^{2-}. The ion is then transferred through the electrolyte to the anode side where it electrochemically reacts. The fuel typically fed to the anode side is either H_2 or CO, to produce H_2O and CO_2 respectively (4). Because of its high operating temperature (800-1000˚C) the SOFC has the advantage to be able to easily integrate with a reformer to the anodic reaction and convert energy from many different fuels, resulting in a great fuel flexibility (4).

4.1 Fuel Cell Fundamentals

A fuel cell is producing electrical work and waste heat from chemical energy in an open system. It can operate continuously, without running down, as long as the electrical potential or electrochemical overpotential is maintained. In other words, by the adding of reactants and removing of the products. The non-equilibrium between the electrical and chemical potentials across the cell will make the charge carriers migrate and charge transfer occurs through the electrode interface. For the H_2 and CO fuels, the electrochemical oxidation reaction taking place at the anode is expressed by Equation 3. Equation 4 describes the oxygen reduction process at the cathode with the O^{2-} working as the charge carrier (25). The overall reaction is described in Equation 5 (26)

Anode: $$H_{2(g)}(or\ CO_{(g)}) + O^{2-} = H_2O_{(g)}(or\ CO_{2(g)}) + 2e' \quad (3)$$

Cathode: $$\frac{1}{2}O_{2(g)} + 2e' = O^{2-} \quad (4)$$

Overall: $$H_{2(g)}(in\ fuel) + 0.5O_{2(g)}(in\ oxidant) = H_2O_{(g)}(in\ fuel) \quad (5)$$

4.2 Thermodynamics

The Gibbs free energy of a system (G) is a thermodynamic potential that can be used to calculate the maximum work that can be performed. In the SOFC the movement of electrons occurs from a higher to lower potential energy and the change in Gibbs free energy of reaction drives an electric current (4).
G is defined as:

$$G = E + PV - TS \quad (6)$$

with:

E	internal energy	[J]
P	pressure	[Pa]
V	volume	[m^3]
T	temperature	[K]
S	entropy	[J K^{-1}]

At isothermal and isobaric conditions, assuming a reversible process, the change in the Gibbs free energy for a reaction [J/mole] is equal to the electrical work done by the system:

$$\Delta^r G = w_{electrical} \quad (7)$$

For a galvanic cell such as a the SOFC the occurrence of a chemical reaction will transport an electric charge from one electric potential to another. As the charge passes a voltage difference, the work is performed. The electrical work $\delta w'_{max}$ done by the galvanic cell is the product of the charge transported and the electric potential difference $\Delta\phi$ and the unit is joule. If dn moles of ions of valence z are transported through a voltage difference $\Delta\phi$ maintained between the electrodes of a cell, then:

$$\delta w'_{max} = zF \times \Delta\phi \times \mathrm{d}n \quad (8)$$

Where F is Faraday's constant= 96485 C/mol (26).

The electromotive force (E) is another important parameter quantifying the potential difference that gives rise to an electric current. If the transport is conducted reversibly this is the electric potential difference between the electrodes of the cell and the equation can be written: (26).

$$\delta w'_{max} = zF \times E \times \mathrm{d}n = -\mathrm{d}G \quad (9)$$

For transporting 1 mole of ions, Equation 9 becomes Equation 10. which is known as the Nernst equation and is the basis for calculating the E value of a specific chemical reaction.

$$\Delta G = -zF\mathrm{E} \quad (10)$$

For a chemical reaction in which the reactants and products do not occur in their standard states the change in Gibbs free energy will be Equation 11, where K is derived from the ratio between the partial pressure for the arbitrary component j, p_j and the standard pressure p_o and R is the universal gas constant (26).

$$\Delta G = \Delta G^\circ + RT\ln(K) \quad (11)$$

The Nernst voltage or the open circuit voltage E_N is the maximum operating voltage, when no current is flowing. The Nernst equation provides a relationship between the standard potential E° for the cell reaction and the open circuit voltage, ideal gas is assumed. E°, that refers to the E under standard state, is a reference state by convenience usually taken as the pure substance at ideal gas conditions, 1 bar pressure and the temperature of the system (4, 26). The equation then is:

$$E_N(T) = E^{\circ}_{\frac{H_2}{O_2 rxn}}(T) + \frac{RT}{zF} ln\left[\frac{P_{H_2(a)} P^{1/2}_{O_2(c)}}{p_{H_2O(a)}}\right] \quad (12)$$

with:

z	Number of electrons involved	
R	Universal gas constant	[J K^{-1} mol^{-1}]
T	Absolute temperature of the cell	[K]
$E^{\circ}_{\frac{H_2}{O_2 rxn}}(T)$	voltage at unit concentrations for H2/O2 reaction at temperature T	[V]

Equation 12 is used to quantify the fuel cell performance and compare it with different setups. It defines the maximum cell voltage of a specific chemical reaction and depicts the fundamental relationship between the thermodynamic quantity and the electrical (4).

5 Ammonia Production

5.1 Nitrogen

Ammonia consists of one nitrogen atom and three hydrogen atoms, where nitrogen is the challenging part in the production. About 80% of our atmosphere consists of nitrogen, found in a state were two N atoms stick together with a triple bond N≡N. This bond is one of the strongest found covalent bonds with a strength of 945kJ/mol at 298K (27). Dinitrogen is a molecule essential for life and for plants to be able grow but it´s not directly accessible to plants and animals. It must be in its "fixed" form like ammonia NH_4^+ or nitrate NO_3^- to be useful (20).

The process of converting the free state of nitrogen in air into nitrogen compounds is known as nitrogen fixation, or nitrogen reduction reaction (NRR). The natural nitrogen fixation, when reactive nitrogen is synthesised to produce ammonia, is an incredibly complicated process spread across different bacterium (28). It´s an exothermic reaction releasing heat and should usually therefor react spontaneously. However significant energy input is required to activate the dinitrogen molecule and enable the reaction process. This is because of the strong triple bond between the N atoms and the activation energy is estimated to 230-240 kJ/mol (29).

5.2 The Haber-Bosch Process

The industrial process of ammonia production took off in the early twentieth century in a time with an increasing need for nitrates, for fertilizers as well as for munitions. As the world started to industrialize the living conditions for

people got better and the populations grew rapidly. The search for a way to industrially produce ammonia lead to great new fields of research such as catalyst promotion, high-pressure chemical engineering, as well as challenges associated with stress corrosion not previously explored (30).

Milestones in the development of the industrial ammonia synthesis includes: 1880 when the equilibrium between ammonia, nitrogen and hydrogen on heating was researched by William Ramsay and Sydney Young. 1904 when ammonia was decomposed as part of the research using a high potential electric discharger. The same year the German chemist Fritz Haber and his assistant measured the ammonia equilibrium at temperatures of around 1000˚C, which was found to be present from 0.102 to 0.024%. The work was then abandoned the year after due to a lack of suitable catalysators for the process. Later on it was developed and preceded under pressure with a good result (31). In 1914 the basis of 3000 publications and patents researched ways to combine atmospheric nitrogen with other elements. (27).

The low conversion-per-pass of ammonia was a great challenge when Haber worked on developing a method. His approach was to start looking at the process with a dynamic method instead of the static view and this became a breakthrough. Based on the new concept of reaction rate he developed a closed process flow and loop operation technology (30). 1913 Haber together with another German chemist Carl Bosch had succeed with building a commercial process. Still today the Haber-Bosch process is being performed and consuming about 1.4% of the world consumption of fossil energy (32). Haber was the inventor who made the breakthrough that laid the foundations for high-pressure chemical engineering, but it was Bosch who subsequently developed it on an industrial scale. They were both separately awarded the Nobel Prize for their work (1918 and 1931) (33).

The great challenge with the Haber-Bosch process is that it's extremely energy dependent. The production is under high temperature (400-500˚C) and pressure (>100 bar), but with an unfavourable position of the thermodynamic equilibrium (29). From a thermodynamic perspective the reaction is favored by high pressure and low temperatures, but the kinetics demands high operating temperature to achieve reasonable ammonia production rates (21). The other challenge is the feedstock for the process which essentially is natural gas. The clean hydrogen gas used for the NH_3 synthesis is mainly generated from the steam reforming process which emits large quantities of carbon dioxide as a by-product (29).

5.2.1 The Catalyst

The ammonia synthesis process is both in terms of amount of energy used and economic cost determined by the performance of the catalyst. Although the proportional cost of the catalyst compared to the total cost of a modern ammonia synthesis plant is negligible. With a needed production rate and given operating pressure, the catalyst then determines the operating temperature range, recycle gas flow and refrigeration requirement(29).

An industrial catalyst for ammonia synthesis should have a high catalyst activity at the lowest possible reaction temperature. This is a crucial quality to let the synthesis process work in the favorable thermodynamic equilibrium situation. The catalyst must also be resistive to poisoning (29).

The fused iron catalyst is one of the most fully studied catalysts in the world. The catalyst emerged from extensive exploratory research and is still the most used catalyst in ammonia synthesis today (34).

6 Low Temperature Ammonia Synthesis

As previously mentioned, the industrial ammonia production is today consuming about 1.4% of the world consumption of fossil energy. The plants are usually big and located near reserves of its domestic feedstock natural gas. The focus in the recent years has been to reduce the energy consumption of the process. Factors affecting the energy flow in the process are for example plant scale and ambient temperature. To recover as much heat as possible from the heat of reaction is also essential and today around 90% is recovered in the loop process (35).

Approaches to find alternative pathways for the reduction process includes exploring photocatalysis, electrocatalysis, chemical simulation and biological NRR. If ammonia could be produced under less demanding conditions, it would also open the possibility for smaller devices to be used to generate ammonia. They could then be used in decentralized manner for local consumption (36).

6.1 Biological Nitrogen Reduction

When trying to find solutions for low temperature ammonia synthesis the best example found so far is the natural synthesis. In nature the ammonia synthesis reaction is done by different microorganism using nitrogenases as enzyme in the process. The biological NRR is performed under ambient conditions and the energy required to overcome the reaction barrier is provided by the hydrolysis of adenosine triphosphate (ATP) (37). Despite more than half a century of intensive research on nitrogenase, its reaction mechanism is still not fully understood. But the available information found in experimental and theoretical studies have still been showed useful in the design of inorganic catalysts (37).

The most commonly found and best studied nitrogenase is the Mo-nitrogenase. In it, the element molybdenum is part of the complex metal cluster that forms the site of N_2 binding and reduction. The other nitrogenase types are V- and Fe-nitrogenase. Where the Mo element is replaced by either vanadium or iron (20).

6.1.1 Molybdenum-Dependent Enzyme

The reduction process of N_2 involving Mo consists of the interaction of two component proteins in the enzyme, the iron (Fe) protein and the MoFe protein. The limiting stoichiometry of the reaction catalyzed by the MO-dependent nitrogenase can be represented by Equation 13 (38).

$$N_2 + 8H^+ + 16MgATP + 8e^- \rightarrow 2NH_3 + H_2 + 16MgADP + 16P_i \quad (13)$$

The interplay with the elements in the reaction is complex and far from understood. The process cycles of the proteins contain of several steps where electrons are exchanged, and ammonia produced. The specific nature of the communication between the Fe and MoFe interface remains obscure. But briefly described the electron-donating Fe-protein transfers the electrons to the metal cluster FeMo cofactor, where N_2 is reduced to NH_3. The binding and activation of N_2 on the FeMo cofactor theoretically and experimentally explain why the entire biological N_2 fixation process occurs under ambient conditions. It can be thought of as an interlocking with the Fe protein 1-electron cycle driving the MoFe protein 8-electron cycle to successively reduced states (37).

An interesting aspect in the Equation 13 is that it's by the use of protons and electrons, and not molecular hydrogen that the reaction occurs. The protons come from solution and the electrons are supplied from another iron-sulfur cluster in the enzyme. There is also a H_2 production in the cycle, concluded from kinetic measurements. Whether this is an integrated part of the reaction pathway or just an inefficiency is under debate (37).

In the research to create a low energy consuming process inspired by the nitrogenase, different methods have been developed. In them the key step has been to promote charge exchange between the catalyst and N_2. It´s been made by designing catalysts with transition metals, constructing oxygen vacancy, synthesize bimetallic compound and so on (39). As one of many good results mimicking this process, Mo (110)-oriented nanofilm was tested by Yang et al. and showed a good ammonia yield 3.09 $*10^{-11}$ mol s^{-1} cm^{-2} at an overpotential of -0.49V vs. RHE (40). Confirming the use of molybdenum as an active catalyst for the ammonia synthesis.

6.2 Electrochemical Ammonia Synthesis

A great amount of research has during the last decades been done to find new ways for ammonia synthesis under less harsh conditions. The electrochemical NRR has the advantage that it can give an overpotential to the process produced by renewable energy sources (5). The electrochemical synthesis can reach an efficiency similar to the conventional Haber-Bosch process and at a high temperature (570 C and 1 atm) the conversion of hydrogen is close to 100% (30). Successful electrochemical ammonia production at ambient conditions from water and nitrogen gas was first reported in 2000 by Kordali et al. (41). This is a great example of an entire energy N_2/NH_3 cycle that can be made completely carbon free, to store and utilize energy.

Adding electricity to drive the ammonia production reaction will decrease the need for high pressure and heat. The electrochemical cell also allows the oxidation and reduction reactions to be separated. This enables a wider range of chemistries and a more selective catalyst. As seen before the mechanism of NRR requires the coupling of multiple electrons and protons. A sustained electron supply is a big advantage in the process as well as the oxidation of water providing both protons and electrons (42). One way to describe the reaction for the electrochemical NRR is by Equation 14, where a total of 6 electrons along with 6 protons are required (28).

$$N_2(g) + 3H_2O(l) \rightarrow 2NH_3(g) + \frac{3}{2}O_2(g) \qquad (14)$$

6.2.1 Reaction Mechanism

The electrochemical reduction of N_2 to NH_3 is a complicated series of steps that involves several intermediates. The inertness in the reaction partly comes from the thermodynamic difficulty of this hydrogenation where some of these intermediates such as N_2H has a very negative redox potential. A high pH is then needed for the reaction in that step to occur (43).

The electrochemical NRR is usually explained by two different reaction sequences on a heterogenous surface, called the Heyrovsky- and the Tafel-type reactions. Since the Tafel-type reaction has a higher activation energy barrier the Heyrovsky-type reaction is usually seen as the dominating one. There are further two types of Heyrovsky mechanisms separated by their different ways of binding nitrogen to the catalytic surface for the hydrogenation. Figure 3 is a basic model for the two reaction mechanisms. In the dissociative mechanism the hydrogenation will take place first when the N≡N bond is broken resulting in individual N-adatoms stuck to the surface. While for the associative mechanism the N_2 remains bound to the surface until the formation of ammonia is completed. At room temperature the associative pathway is favorable due to the difficulties in breaking the triple bonds of N_2 and its represented in the reaction mechanism in enzymes. While for the Haber-Bosch process the reaction mechanism is dissociative (28).

The most exergonic step in the reaction mechanism is usually also the potential determining step. For the associative process this has been showed to be the adsorption of molecular nitrogen and the first proton transfer step. For the dissociative mechanism it's instead the N_2 splitting that will influence the reaction rate the most (7).

6.3 The Chemistry of Dinitrogen

As mentioned before the two N atoms in N_2 is bound together by an extremely strong triple bond. An N atom has five valence electrons in the 2s and 2p orbitals and three of them are unpaired. When coupled the orbitals is divided into two σ and two π bonding orbitals and four anti-bonding orbitals, see Figure 4 (39). There is a large gap between the highest occupied molecular orbital to the lowest unoccupied molecular in N_2 and a high ionization energy (15.58eV) that prevents electron transfer.

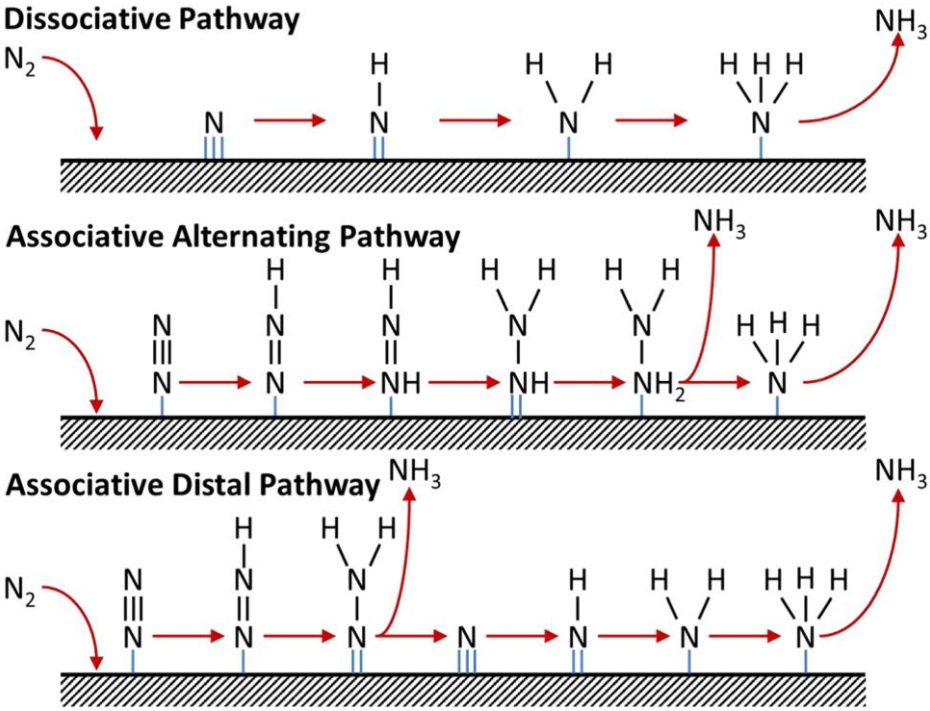

Figure 3: Reaction sequences of the electrochemical NRR on a heterogenous surface. Reproduced with permission (36) Copyright 2016, Elsevier.

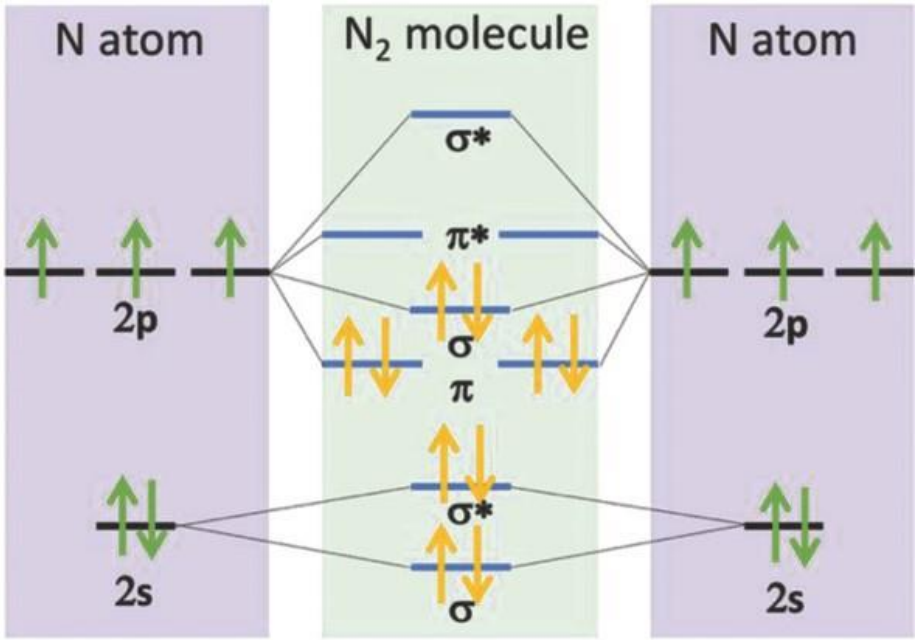

Figure 4: The diagrams of N atomic orbitals and their hybridization. Reproduced with permission (39) Copyright 2018, Copyright Clearance Center

6.3.1 Adsorption and Activation of Nitrogen

The first step in the NRR is the adsorption of N_2 onto the catalyst. As the concentration of dissolved N_2 has seen being a rate-limiting factor, bubbling N_2 gas and thus generating a dynamic gas-liquid-solid interface will improve the reaction result. Fe and Mo have been found to exhibit the ability to form metal-nitrogen bonds, which mimics the nitrogenase. These bonds are with their established electronic channels by bonding beneficial for the next step in of electron donation from the metal to N_2 (39). N_2 adsorption could also be prompted by vacancy (44).

The rate limiting step in the NRR can also be the activation of N_2, which is strongly associated with the N_2 chemical adsorption process (45). The bond length N-N of N_2 at the facet of a catalyst differs and the results are the degree of N_2 activation established. With a longer distance between the atoms the molecule is referred to "being activated" at a higher degree. Some transition metal complexes can bind N_2 without changing the length and the energy of N-N bond at all. However, for other metal complexes, the N_2 acquires different degrees of activation through coordination with the metal centers. N_2 can also be chemisorbed and activated on N_2 vacancy as well as oxygen vacancy, by combining with the nearest metal atoms. The back transfer of charges from the vacancy to the N_2 in this process is the possible reason for the N-N bond activation (39).

7 Catalysts

A catalyst's purpose can be defined as to increase the rate of a chemical reaction without being consumed itself. In the industry they are widely used today to accelerate the rate of reaction towards equilibrium, with the purpose to improve the process economics. Many industrial chemical processes rely on catalysts to lower the activation energy of reactions and the performance of the catalyst is therefore essential for the overall process efficiency. Most of the catalysts used today are solid and operate heterogeneously in processes such as combustion, catalytic cracking in refineries, petrochemistry or ammonia and methanol production (46).

The activity of the catalyst in a reaction is determined by the rate at which the reaction proceeds on the catalyst volume or mass charged to the reactor. The yield of products and by-products from the process can be quantified. An important measurement is the selectivity that shows the proportion of useful product obtained from the amount of feedstock converted. With a catalyst boosting the reaction activity the great gain is that a better selectivity can be achieved at milder operation conditions (46).

General characteristics affecting the catalyst activity in a reaction are mainly the catalysts morphology, crystallinity and the density of surface-active sites. To have many and easily available active sites is the key as well as to enable a good mass transfer over the catalyst. Stability is also of great importance where some catalysts can be regenerated in situ (46).

8 Designing a Nitrogen Reduction Electrocatalyst

The development of an efficient NRR electrocatalyst will offer a great pathway in industries to produce fuels and value-added chemicals. In the past few years there have been a great development and optimization of electrocatalysts for reactions such as the hydrogen evolution reaction (HER), oxygen evolution reaction (OER) and oxygen reduction reaction (ORR) (47). N_2 fixation has been studied for more than 100 years, but an optimal catalyst has still not been found and more theoretical and experimental research is still needed (30). When considering the material design, an efficient NRR electrocatalyst should possess desired composition, crystal structure and surface properties as well as good electrical conductivity to facilitate electron transfer (47).

As for the iron catalyst in the Haber-Bosch process the catalytic components are usually mixed with other materials for promoters or support. These supporting materials could provide a porous framework and enhance the lifetime of the catalyst. This for example by adding components that during the sintering can interact to avoid the in other case occurring loss of active surfaces, or by absorbing traces of poisons (46). Using carbon material as the supporter and separator is one good example where a preferred structure can be obtained. This thanks to the carbon structure with its excellent electrical conductivity and chemical inertness (48).

The more active sites for the catalytic reaction the better catalytic capability and for this a high surface area is beneficial. For NRR one successful approach has been to use black silicon nanowires. Wires are introduced on the surface of planar silicon wafers, and as the surface feature sizes are reduced to a few nanometers, enough sites for the catalytic Au loading are provided, thus achieving efficient solar light driven conversion of N_2 to NH_3 (39). The catalyst production process technique and properties also have an effect on the size of the surface area (49).

Many forms of vacancies (oxygen, nitrogen, sulfur vacancy) has also been showed to boost the activity of NRR. This effect is considered due to the high dispersion of N_2 fixation over vacancy. Usually highly dispersed vacancy can make full use of the interface to enable catalysis of more nitrogen molecules at the same time. A new approach in the catalyst design is a single atom construction. Some different works have been performed in this area and highest efficiency of electrocatalytic conversion of N_2 has been reached when having a good dispersion of atomic Au cluster. It is expected that maximum atom utilization can be achieved by continuously minimizing the size of the Au nanoparticles (39).

A big challenge in the design of a new optimized nanostructured catalyst is the importance of a long-lived material. When looking at designed vacancies the control of the features and stabilization is extra hard to achieve. Towards this requirement, the fabrication of a suitable structure enabled nanostructured catalyst to refresh active sites should be devoted more efforts (45).

8.1 Selectivity

The greatest challenge when applying a potential to boost the NRR in an aqueous solution is the competing hydrogen evolution reaction (HER). It´s the formation of hydrogen gas H_2 from water and with the theoretical potential for H_2 formation being very close to the theoretical potential for NRR it's a reaction that's extremely hard to avoid. Li and co-workers (50, 51), studied the mechanism for nitrogen electroreduction to ammonia in an alkaline electrolyte to explain the phenomenon of their catalysts showing good activity but a low Faradic efficiency (FE). Their results showed that in addition to air and nitrogen gas, water is necessary to achieve high ammonia production efficiency. They also tested a range of applied overpotentials and found that the efficiency increased with an increased potential up to a peak level and thereafter it decreased. The peak level coincided with the theoretical potential for water electrolysis. These results point out a mechanism that uses the protons and electrons in the solution to produce hydrogen gas in a bigger extent than to form ammonia. If the reaction kinetics for the hydrogen formation on the catalyst surface is faster than for the NRR the FE of the process will be low (48).

To optimize the catalyst for both activity and selectivity is the primary challenge in the electrochemical NRR. Theoretical models point out the key issue among all metals examined, that hydrogen atoms will preferentially adsorb over nitrogen atoms (52). Surface properties that prefer strong binding with N-adatoms to H-adatoms together with good electrical conductivity will promote a suppression of HER and enhance the efficiency in addition. The proton accessibility in the electrolyte is another important tool to suppress the formation of H_2. With the aqueous base containing a lot of protons, limiting the access to them is hard. But varying the composition and the choice of the electrolyte has shown to be effectful (53). Another good approach was the use of a hydrophobic layer on the electrode to suppress water electrolysis while still allowing N_2 to pass through (54). To increase the concentration of N_2 in the solution has also been proved to successfully suppress HER (53).

Nanoscale Design

In the search for new materials to components exposed to high pressure and harsh/acidic environments, nanoscience has risen as a research field of great interest. To create more efficient and persistent electrochemical cells the materials are one of the major challenges. The ability to keep precise control over size and composition of the material, further with the possibility to assemble them into large structures has been showed to offer great potentials. It has been discovered that these materials, usually in the scale of 1-100nm gain unique sets of properties comparing with the traditionally used industrial materials today (8). The main research fields are nanoparticles, nanocrystals, nanofibers, nanotubes and nanocomposites with well-defined structural features. For industrial application the goal is to produce high purity powders with fine particle size, usually with small aggregation and with low production cost. In the science of catalysts the construction of two- or three-dimensional nanostructures can expose the active sites and drastically enhance the catalytic activity (39).

In advancing fuel cell technologies nanomaterials can play a crucial role. Some of the main challenges for further commercialization cover poisoning of the anode from hydrocarbon fuels as well as carbon deposits and durability problems. Nanostructured design of cathode and anode materials can help avoiding these problems. Also nanocomposites offer great design advantages in which one component can offer high electronic conductivity and the other component high oxide-ion conductivity (13).

For the NRR there have been great examples of nanodesigned catalysts that contributed in overcoming the kinetic limitations of the reaction (39). The catalytic performance can from a nanoscale perspective be controlled by properties such as phase, electronic structure, morphology and surface structure of the catalyst (52). The paper published by Yang et al. of (110)-oriented Mo nanofilm catalyst also demonstrates the successful nanodesign approach (40). In another paper tetra hexahedral gold nanorods (THH Au NRs) with exposed facets produced by Yan and co-workers resulted in a high production rate of 1.648 $\mu g\ h^{-1}\ cm^{-2}$ but with a low FE of 4% at -0.2 V (55). A much better FE was obtained from hollow gold nanocages (AuHN Cs) by Nazemia et al. with a FE of 30.2% and the highest ammonia yield at -0.5V of 3.9 $\mu g\ h^{-1}\ cm^{-2}$, thanks to the better exposure of the active sites (56).

8.2 Materials

There are three categories of electrocatalysts for NRR that mainly have been reported including noble metal electrocatalysts, non-noble metal electrocatalysts and metal-free electrocatalysts (47).

Noble metals have been dominating as electrocatalysts for a wide range of reactions because of their ability to provide strong binding for a wide range of reactants and their good electrical conductivity. Most widely explored noble materials for NRR are Ru, Rh, Au and Pt (57). The main disadvantage with the noble metal-based catalysts is the high prize and the accessibility of the materials. To find inexpensive alternative electrocatalysts is therefore critical for large-scale industrial applications (6).

8.2.1 Transition Metal Catalysts

Low cost, earth abundance as well as their structural advantages, has made transition metals a dominating catalyst material for NRR. The beneficial property of this category is that the d orbitals of transition metal ions are incompletely filled with electrons. This results in very useful electron chemistry characteristics: easy exchange of electrons from other species and an ability to activate strong bonds (39). The structural characteristic for this group of metals is the fact that their (n-1)d subshell has almost the same level of energy as its outer shell (n). Thus, this element reacts through the electrons of its outside shell (n) and the electrons of its (n-1)d subshell. Compared to a main group of elements such as carbon, nitrogen etc., that reacts only through the electrons of its outside shell (n). This phenomenon of the transition metals is called Π-back bonding and it's a phenomenon in which electrons move from an atomic orbital on one atom to an appropriate symmetry antibonding orbital on a π-acceptor ligand. It enables many synthetic applications with one being alleviation of kinetic issues for N_2, leading to good binding of nitrogen and efficient NRR (58).

Possible transition metals have been theoretically evaluated for ammonia production with the coincidental HER reaction by Skúlason et al. (7). Density functional theory (DFT) calculations were performed for the adsorption energies of all intermediate states for the flat and stepped surfaces in the Heyrovsky Mechanism. The adsorption step being a rate determining step for the NRR. With the activation energy scaled to the free energy difference in each elementary step of NRR, the free energy change could be estimated. The result is presented in a so-called volcano plot, see Figure 5. In it, the selectivity and catalytic activity can be visualized and compared between different materials for a chosen reaction. Showing the onset potential for the formation of NH_3 and the N-adatom vs. H-adatom surface binding. From this plot a better understanding of the reaction mechanism can be achieved and it's a great tool for showing promising transition metals for further NRR electrocatalyst design.

In Figure 5, the black line stands for a flat surface and the red line is for a stepped surface. Grey area indicates the conditions under which the surface will likely be covered with H-adatoms. While the white area is where N-adatoms is preferentially adsorbed instead. This result shows that flat transition metal surfaces of Sc, Y, Ti and Zr should be able to reduce N_2 to NH_3 in good result to HER, since the N-adatoms would bind more strongly (7).

8.3 Oxides and Perovskite Type Catalysts

With pure transition metal catalysts in an electrochemical NRR the NH_3 yield is quite low while the reactions require relatively high applied voltage to occur. Metal oxides offer a solution to this providing a beneficial structure for the reaction process. They are stable materials, preventing the oxidation of the transition metal which normally is a weakness at high temperatures in the presence of oxygen (9). The pioneering work was reported by Schrauzer and Guth when they showed that Fe-doped TiO_2 efficiently reduced N_2 gas into NH_3 and a small quantity of N_2H_4 (59). This has inspired to a lot of further research with transition metal doped TiO_2 (39). Another example is the Fe_3O_4 nanorod on a Ti mesh (Fe_3O_4/Ti) with a FE of 2.6% and the highest ammonia yield of $5.6*10^{-11}$mol s^{-1} cm^{-2} at an applied potential of -0.4V vs. RHE (60). This shows a promising opportunity with metal oxide catalysts in the search for a way to reduce the mass and enhance the performance in the NRR.

With metal oxides offering a stable and active catalyst, flexibility can further be promoted by adapting a perovskite material structure. This will enable a great control over the catalyst properties and the unique possibility to find an optimized electrocatalyst. Perovskite oxides with the general formula ABO_3, are isomorphic solids, able to fit a large number of cations into both the A and B positions. See Figure 6, where an ideal perovskite structure is illustrated for $SrTiO_3$. The great advantage is that the perovskite structure can tolerate substitutions at both cations sites with the crystal structure being unaltered. Practically all the metals are stable in the perovskite lattice (9).

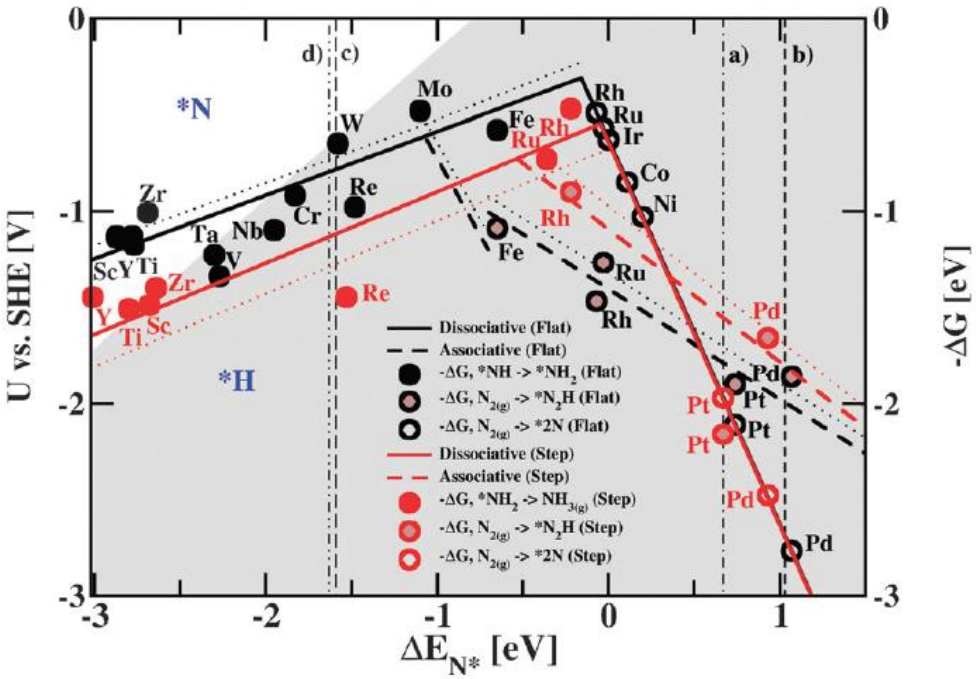

Figure 5: Volcano plot of the selectivity and catalytic activity for NRR on different transition metal surfaces. Reproduced with permission from Royal Society of Chemistry (7) Copyright 2012, Clearance Center.

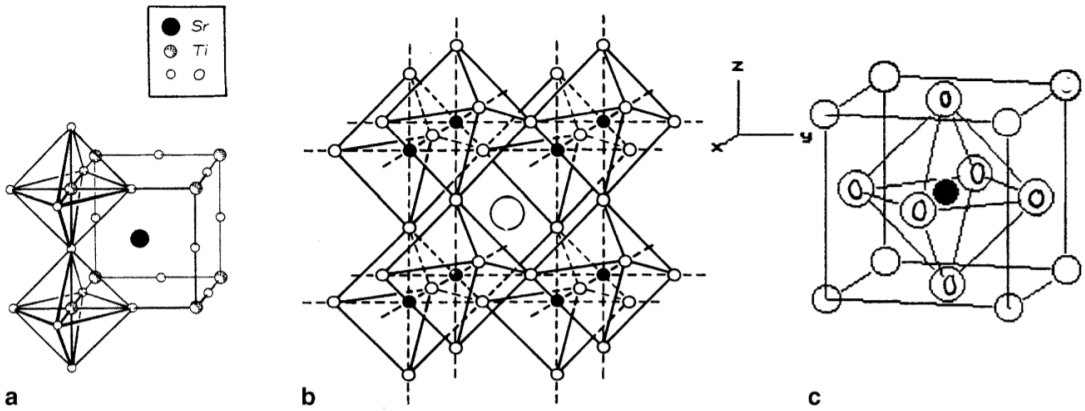

Figure 6: The ideal perovskite structure, illustrated for $SrTiO_3$ in three different ways. Reproduced with permission from Taylor & Francis (61) Copyright 2000, Clearance Center.

The inorganic perovskite-type oxides are used in fuel cells as well as electrochemical sensing. In catalysis perovskites can be used in electrocatalysis, auto-exhaust treatment and catalytic combustion. The major advantages is their thermal stability and that the oxygen and cation non-stoichiometry can be tailored in a large number of perovskite compositions to achieve desired designs for a variety of reactions (62). The only found previous study of a perovskite catalyst for NRR is by Wang and co-workers who synthesized $LaFeO_3$. The result was a NH_3 production rate of 250μ mol g^{-1} h^{-1} under simulated sunlight and with acid treatment (63).

8.3.1 Crystallography of Perovskite Materials

The perovskite lattice consists of small B cations within oxygen octahedra, and larger A cations which are coordinated by oxygen. Many of the materials exhibit the orthorhombic Pnma or Pbnm distorted structure at room temperature. This structure is double the size of the ideal cubic perovskite unit cell. It can also be found in a further distorted structure as rhombohedral structure or hexagonal depending on the size of the A and B cation. Although abrupt crystallographic changes by different radius of the cations, the lattice or internal energy will not be noticeably affected (64). The A cation is generally catalytically inactive while the B is the active component in the structure. Proper combinations and partial substitution of A- and B-site cations can give rise to special B-site cations and/or oxide ion vacancies. Introduction of such lattice defects cause modifications to the chemical or transport properties of the oxides which affects the catalytic property (65).

A high crystalline structure of the perovskite material catalyst improves the catalytic activity. One benefit is the small surface area presented with the high crystallinity as showed by Evans and co-workers who successfully produced a perovskite supported catalyst with AuPt nanoparticles for glycerol oxidation reaction (49). The high crystalline structure of the material can also promote the charge transfer from the catalyst's bulk to its surface and boost the NRR (57).

In catalytic research the knowledge of the correlation between the catalytic and solid-state properties plays a crucial role. To be able to generalize such parameters experimental data is the key. It has for example experimentally been showed that the orientation of the crystal phase can enhance the catalytic performance. The crystal plane orientation of the samples also result in various different surface features and different catalyst activity. The result with different rates of formation of ammonia on the surface in different cases shows that the processes are shape selective and crystal structure sensitive (40). It has also been showed that the catalytic performance is affected by the crystal structures (57) as well as the size of the crystals (66).

8.3.2 Oxidation States and Doping

The oxidation state tells the actual number of electrons that atoms in the material contain. During the production process the oxidation state of the components can be affected and result in extra electrons being lost or gained. For perovskite materials, partial substitution of the B cation can improve both the structure stability and the catalytic behavior. Substitution of the A cation with a different oxidation state will also affect the oxidation state of the B-site

cation and might cause structural defects such as vacancies. The mobility of the lattice oxygen determines the mechanism of the catalytic oxidation reaction (67). Up until now, not many studies of the solid-state properties and catalytic activity for NRR have been conducted. Instead, results can be studied from other oxidation and reduction reactions with perovskites catalysts.

The CO oxidation is one reaction widely studied. Results have showed that doping the perovskite catalyst can increase the density of oxygen vacancies and regulate the distribution of B-site oxygen states (67). Also, to investigate the different phase states of the components in the catalyst surface and the effect on catalytic reaction rate is important. By varying the oxidation state of the B^{3+} ions it can be determined how the N_2 is bonded to the catalyst atom, in what phase and then correlate this to the reaction rate (65). The importance of the lattice oxygen was also showed for a NO reduction process. It showed that perovskites that can easily release an oxygen will be active for reduction reaction. Cation vacancies that provide weakly bound oxygen to the surface, favour both the formation of oxygen vacancies and NO reduction (65).

8.4 Lanthanum Chromite Oxide

$LaCrO_3$ is a ceramic material that has started to get more frequently used in heterogenous catalysis. The compound structure consists of the rare-earth ion (La^{3+}) occupying the A site with the oxygen ions and the transition metal (Cr^{3+}) as the B cation in octahedral coordination (68). It got attention early in the field of material science because of its many good properties such as high melting point (>2400˚C), high electroconductivity, small temperature coefficient of resistance and high stability against oxidation and corrosion (69). Cr^{3+} ions have previously been reported by Chang et al. to show a strong capability to thermodynamically capture N_2 (70). The results explained by electron donation and unsaturated transition metal sites was a breakthrough in adsorption-based technologies for NRR catalyst design.

For fuel cell application $LaCrO_3$ is a commonly used interconnect material because of its high electronic conductivity under fuel and oxidant atmosphere and adequate stability in fuel cell environment. It's ability to withstand high temperatures also makes it a good material for heating elements (71, 72).

Methodology

1 Material Production and Characterization

1.1 Hydrothermal Synthesis and Co-Precipitation

The synthesis and characterization of nanostructured materials is a field with a growing interest from researchers and engineers today. The ways to synthesise nanoparticles commonly reported include solution processes, solid-solid or solid-gas reactions. The properties of the produced nanopowders such as the crystalline structure, amorphous structure, crystalline size, purity, specific surface area and particle agglomeration depend on the adopted technique and processing parameters (8).

Many of the popular processing methods such as solid-state reactions are built on undesirable circumstances. This includes the use of high temperatures, toxic organometallic precursors, or many complicated reactions steps (73). The solvothermal process offers a simple and economical alternative to this. The method takes advantage of the increased solubility and reactivity of metal salts at elevated temperatures and pressures. When water is used as the solvent it's called a hydrothermal synthesis. It's performed by putting the solvents in a sealed vessel (bomb, autoclave, etc.) and the temperature is thereafter increased. In the vessel the autogenous pressures will increase as a result from the heating, but without bringing the solvents to its critical boiling point (74).

Before the heat treatment the co-precipitation method is suitable to use for mixing the chemicals in the right ratios. For perovskite materials this is a convenient way from which all compounds can be synthesized from metal nitrate and carbonate salt (75). The steps include aqueous solutions of the metal salts, that are precipitated with an alkali. A support material can also be added as a powder. When the precipitate has formed and settled, it is filtered and washed before drying. The remaining material is then calcined to decompose the hydrates and carbonates and the resulting catalyst will contain a high concentration of base metals (46).

As the hydrothermal treatment is proceeded, trapped bulk water is removed from within the structure of the material. The materials are dissolved and then recrystallized in the closed system (73). The use of these different solvents in the chemical reaction is essentially to lower the pressure and temperature for the reactions to occur. Soft solution processing has the advantage over solid state reactions with lower temperatures for crystallization of the material since the diffusion distance for reactants are shorter (68). The products of solvothermal reactions are usually crystalline and do not require post annealing treatments (74). Other ways to produce sinterable $LaCrO_3$ perovskite powders are for example by the sol-gel synthesis (76) or by the combustion method (77).

1.1.1 Particle Size and Morphology

The control of particle size and morphology during the hydrothermal process depends on the reaction interval, temperature and alkalinity of the solution. Milder conditions can result in more uniform and mono-disperse particles (78). It's also advantageous to avoid the formation of $La(OH)_3$ phase in the particles, since the solubility of $La(OH)_3$ is decreased at higher temperature. But at the same time, the growth and recrystallization speeds of $LaCrO_3$ crystals are increased with increasing temperature (79).

The effect of alkalinity in the solution is associated with the perovskite-type structure and the properties of the ions. The hydrothermal activity of the B-cations will significantly influence the synthesis due to its position in the perovskite structure. In different alkaline environments the cations will show different stability which will have an effect in the final structure (79). Huang et al. showed the effect of different concentrations of a the cosolvent urea in the solution and the result with a shape evolution of the particles from cubic to round (80). The cosolvent effect the reaction by stabilizing different crystal forms, it can stabilize octahedral crystals over the usual cubic form for example.

Under the liquid phase conditions, the final crystal shapes are mainly determined by the relative speed of growth in each crystal orientation. Usually the higher the surface energy of the crystal plane, the easier it is to diminish this plane in the final shape of the crystal. This is because high surface energy is needed to keep the surface stable and by diminishing this energy with other ion attachments, there is greater crystal growth speed in this direction (78).

1.2 Sintering

As a final treatment the material will be sintered in a furnace. The aim of this process is to get a denser microstructure and avoid/eliminate the remaining pores in the structure. The microstructure will change with the elevated temperature and the relative density will increase. At some maximum point though the trend might turn, and the relative density start to decrease. This phenomenon has been associated with the loss of Cr for the case of $LaCrO_3$ perovskite. Partial decomposition of lanthanum chromite under oxidizing conditions at high temperature for $LaCrO_3$ was identified by Rivas-Vázquez et al. as the reason (81). This can result in a great amount of porosity in the material. Doping has showed a positive effect for improved sinterability (10).

1.3 Half-Cell Electrochemistry

To examine the prepared catalyst material and its contribution to the NRR, a half-cell method is used. This is a quick and cost-efficient way to test components as catalysts when also eliminating the possible interference from other reactions. The NRR can be electrochemically tested and the effects that the operating conditions have on the reaction can be examined (82). The NRR consist of two redox half reactions and can therefore be split into two half-cells where each of them has only one electrochemical interface. Typically N_2 gas will be bubbled at the cathode chamber and hydrogen, from the water or provided as gas, can transfer as H^+ in between the chambers (14). The overall reaction is (36):

$$N_2 + 3H_2O \rightarrow \frac{3}{2O_2} + 6e^- \rightarrow 2NH_3 + 6OH^- \quad (15)$$

Half-cell testing is usually conducted in a three-electrode system containing a working electrode (WE), counter electrode (CE) and reference electrode (RE). The working electrode is the catalyst coated material, made of for example glassy carbon paper or other stable materials. The counter electrode which is used to close the current circuit is made of an inert material like a Pt wire, Pt foil, or graphite rod. The reference electrode is typically a standard or normal hydrogen electrode or an Ag/AgCl electrode (82). In-between the two cells a membrane is placed to separate the two electrolyte solutions. To maintain the electrical contact between the cells while avoiding unwanted crossover of specific ions, various types of porous materials are normally used. The selectivity of these membranes is therefore crucial. A commonly used material is Nafion, a polymer proton exchange membrane with great mechanical and chemical properties. The polymer proton exchange membranes should have a selective proton conduction at low temperature and insulate to electrons (14).

1.3.1 Reference Electrode

The term electrode is in its strict definition referring to the interface where the redox half-reaction occurs in an electrochemical system. Although it's often used to describe the whole device with the electronic conducting material, its support and the electric connection. A reference electrode is a bit more complex. Containing an electrochemical system with a known stable potential it's providing a reference measurement and a porous material ensures the contact with the cell's electrolyte (14).

The reversible hydrogen electrode (RHE) is a practical electrode "standard". The term refers to a hydrogen electrode immersed in the electrolyte solution actually used un the measurement cell. It's a useful unit to compare results from different electrochemical measurements. Various electrochemical half-cells have therefore been developed as references for potential measurements in electrochemical systems such as hydrogen electrode, silver chloride electrode (AgCl) and calomel electrode (Hg_2Cl_2). Ag/AgCl is a reference electrode commonly used, normally saturated in KCl to keep the potential stable. The purpose of the saturation solution is to form a layer on the electrode to stabilize it during the process. The measured potentials vs. Ag/AgCl can then be converted to the reversible hydrogen electrode (RHE) scale (14).

1.4 Electrochemical Testing

Time, current and voltage are the main parameters in an electrochemical experiment. To record data measurement devices such as voltmeters and ammeters are used, as well as sources for energy supply such as electric current source and voltage source. A more high-performance measuring system than a normal voltage generator controlling the voltage between the systems two terminals, is the potentiostat. A setup with three electrodes is then used, where the potentiostat controls the voltage difference between the WE and the reference (14).

1.4.1 Amperometric Measurement

The technique when measuring the current as a function of an independent variable, usually time or electrode potential it's called amperometry. A subclass of this is voltammetry, when the current is measured by varying the potential applied to the electrode. To study the electron transfer kinetics and transport properties of electrolysis reaction a linear sweep voltammetry (LSV) test can be applied where the potential will be changed in steps. This is an efficient method to for example distinguish the most promising potentials for NRR while avoiding the competing HER (12). When applying a time-depending potential to an electrochemical cell the resulting current plot provides a quantitative and qualitative information about the species involved in the oxidation or reduction reaction (14).

Another amperometric detection technique to determine the degree of catalytic activity at a given potential is the Amperometric i-t curve. A constant potential is applied, and the current is recorded as the function of time. Parameters are the initial potential, data sample interval and sensitivity scale (12).

1.5 Ammonia Determination

A technique used to determine the concentration of a specific chemical in a solution is colorimetry. Nessler's method for ammonia, introduced 1856 is an early example of a colorimetric analysis (83). The theoretical basis is simple, using coloring chemicals with a clear difference in color intensity for different concentrations of the tested sample. Nessler was able to determine the concentration of ammonia by visually comparing the color of the sample (HgI_2 and KI as an alkaline solution mixed with the dilute solution of ammonia), by visually comparing the color of a sample to the colors of a series of standards (83).

A widely spread method to determine ammonia in a solution is based on a reaction with phenol and hypochlorite, in which a blue coloured indophenol compound is formed. Different catalysts are used for the reaction, especially sodium nitroprusside and potassium ferrocyanide. The method is very sensitive and can be applied to many types of samples (84). An optional method is to use sodium salicylate as a substitute for indophenol. The aim with this substitute is to prevent the formation of the poisonous ortho-chlorophenol (85).

To quantitively distinguish the amount of formed solution spectrophotometry is a commonly used method. It's based on the phenomenon that every chemical compound absorbs, transmits, or reflects light (electromagnetic radiation) over a certain range of wavelength. It measures the amount of photons (the intensity of light) absorbed after is passes through the sample solution. With the spectrometer, the amount of a known chemical substance (concentrations) can be determined by measuring the intensity of light detected at a specific wavelength (83).

1.6 X-Ray Diffraction

X-Ray Diffraction (XRD) is a great tool to investigate the fine structure of matter. In the crystal lattice the atoms are arranged periodically, so by X-ray the crystal structure can be determined by analysing its atom positions and the

unit cell (86). The prepared material should firstly be milled to a fine particle size. A large number of crystallites should contribute to the diffraction process for a greater accuracy. The X-rays will diffract through the crystal and into a detector. The beam and the detector are rotated through a range of angles (called Braggs angle). By this rotation intensity peaks will be seen in the X-ray spectra and from that the crystals in the material can be identified and the surface facets can be indexed. The orientation of planes in a lattice is usually represented symbolically by the Miller index. The angular positions of the diffraction lines indicate the different planes in the crystal. The amount of the atoms can then be deduced from the relative intensities of the diffraction lines (86). This can determine the bulk phases in a catalyst and the crystalline size (87).

1.7 Transmission Electron Microscopy

When characterizing a material another important aspect is the size and the distribution of the phases. This can be seen in a Transmission Electron Microscope (TEM), which provides atomic-resolution images of materials and their defects. TEMs are the most powerful electron microscopes with the resolution of particles in 1nm scale. Electrons in high speed zoom through the specimen and out the other side, where coils focus them to form an image. The material is prepared in a thin slice of specimen very carefully and then it sits in a vacuum chamber in the middle of the machine (88). The specimen can be either self-supporting or resting on a support grid, for example a carbon film. The crystallographic data from specific locations in electron-transparent specimens are then used for structural identification (89). For single crystalline grains a uniform set of lattice planes will be seen, and the lattice distance can be related to planes in the structure. In other cases the interface between different crystals/grains can provide valuable information (90).

1.8 X-Ray Photoelectron Spectroscopy

For all solids, the composition of the surface layer is usually different from the composition of the bulk. X-ray Photoelectron Spectroscopy (XPS) is a useful tool to identify the oxidation states of the species at the surface. Thru this the surface composition and valence states of the material is investigated, and the appearance and oxidation state of the atoms determined (91).

Exposing a sample to X-rays of sufficient energy will result in electrons in specific bound states to be excited. As electrons are in orbitals farther from the nucleus, less energy is required to eject them, so the binding energy is lower for higher orbitals. By showing the energy of electrons emitted from a material, XPS allows for the composition of a material to be determined. The ejected electrons can be collected in vacuum and their kinetic energy then measured. This will produce an energy spectrum of intensity versus binding energy for the material. Each prominent energy peak on the spectrum corresponds to a specific element. Besides identifying elements in the specimen, the intensity of the peaks can also tell how much of each element is in the sample. Each peak area is proportional to the number of atoms present in each element (91).

1.9 Scanning Electron Microscopy

Just like any microscope the aim of the Scanning Electron Microscope (SEM) is to enlarge small features not visible to the human eye. Instead of light it uses an electron beam to form images in optical light microscopes. An electron beam of high energy is scanned on the sample surface and the surface morphology can then be visualized. A specific sample preparation is not required, which contributes to the popularity in using this method (92). To get information of the material composition an X-ray detector can be used in the SEM and Energy Dispersive X-ray Spectroscopy (EDS) is the most commonly used. As the specimen is exposed to the electron beam, characteristic X-rays will be excited. As they are collected by a detector their energy and intensity distribution can be measured and the detection of most elements will be possible (93).

2 Experiments

The experiments were conducted in three steps; the preparation of the material, electrochemical testing and characterization.

2.1 Hydrothermal Synthesis

$LaCrO_3$ nanoparticles were prepared by the co-precipitation method following previous of work of Rivas-Vázquez et al. (81), but with a different heat treatment. For a schematic schedule of the hydrothermal synthesis, see Figure 7 and for the chemicals used, see Table 1. To begin with solutions with the metallic salts ($Cr(NO_3)_3$ (99.0%), $LaCl_3$ (99.0%)) were weighted and dissolved in different beakers containing deionized water. Both salt solutions each had a concentration of 0.05M. The (alkali) precipitating solution sodium hydroxide (NaOH (98.0%)) was prepared with a concentration of 0.5M.

Table 1: Chemicals used in the hydrothermal synthesis.

Chemical	*Molarity [mol/liter]*	*Molar mass [g mol^{-1}]*	*Mass [g]*
$Cr(NO_3)_3 \times 9H_2O$	0.05	400.15	5.00
$LaCl_3 \times 7H_2O$	0.05	371.37	4.64
NaOH	0.5	40	5.00

The mixing was then carried out with 237.5ml of the NaOH solution poured in a beaker together with 250ml of the solution of chromium. The formation of an opaque whitish green precipitate appears when the solutions get in contact. The solution was magnetically stirred for 30min. A vigorous stirring of the mixed solution will lead to the dissolution of the preliminary precipitated gel of $Cr(OH)_3$.

Finally, the co-precipitation of the complex gel was carried out by the addition of the same volume (250ml) of the lanthanum solution. A molar composition matching the stochiometric ratio for $LaCrO_3$. The complete solution was magnetically stirred for 10min. The coprecipitated gel was then separated into several tubes and centrifuged in steps. The separated water was removed from the gel and the solution was reduced to a volume of 50ml, see Figure 8 (a). A volume of 25ml was then poured into a hydrothermal autoclave reactor (50ml capacity).

The heat treatment was carried out as the autoclave was heated at a temperature of 200˚C for 20h. After the treatment, pieces of precipitates were showing in the solution. It was well washed several times with deionized water and then put to dry in an oven at 100 ˚C for 9 hours, see Figure 8 (b).

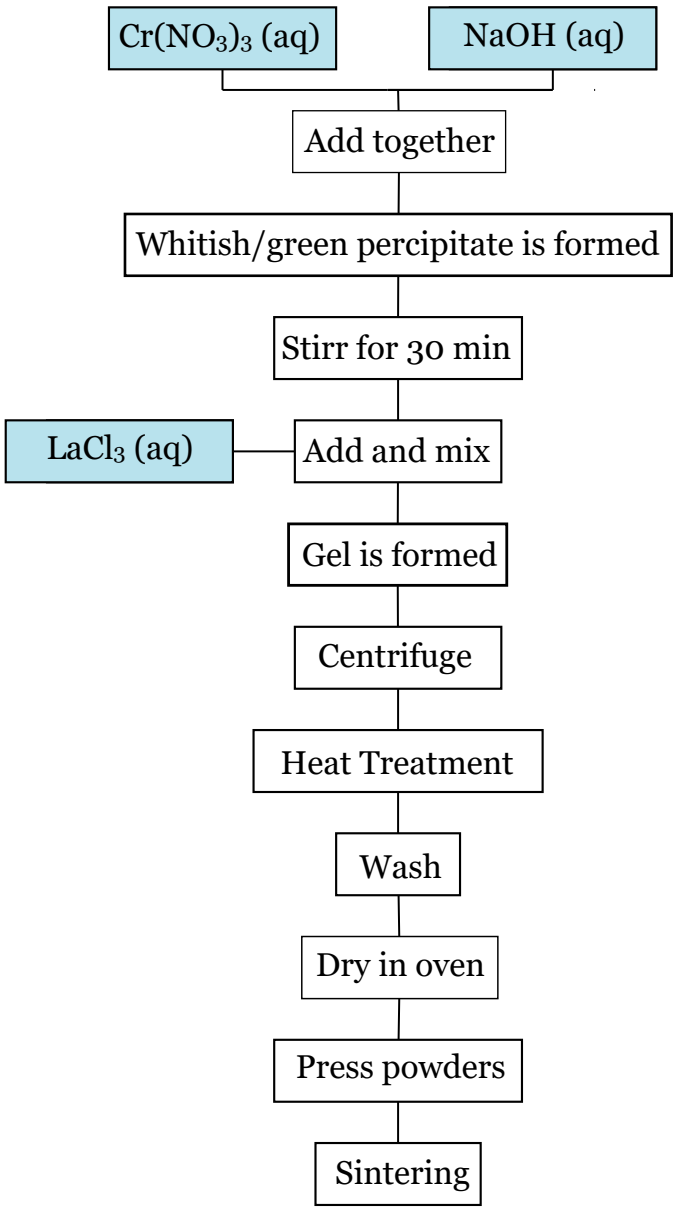

Figure 7: Schematic schedule of hydrothermal synthesis

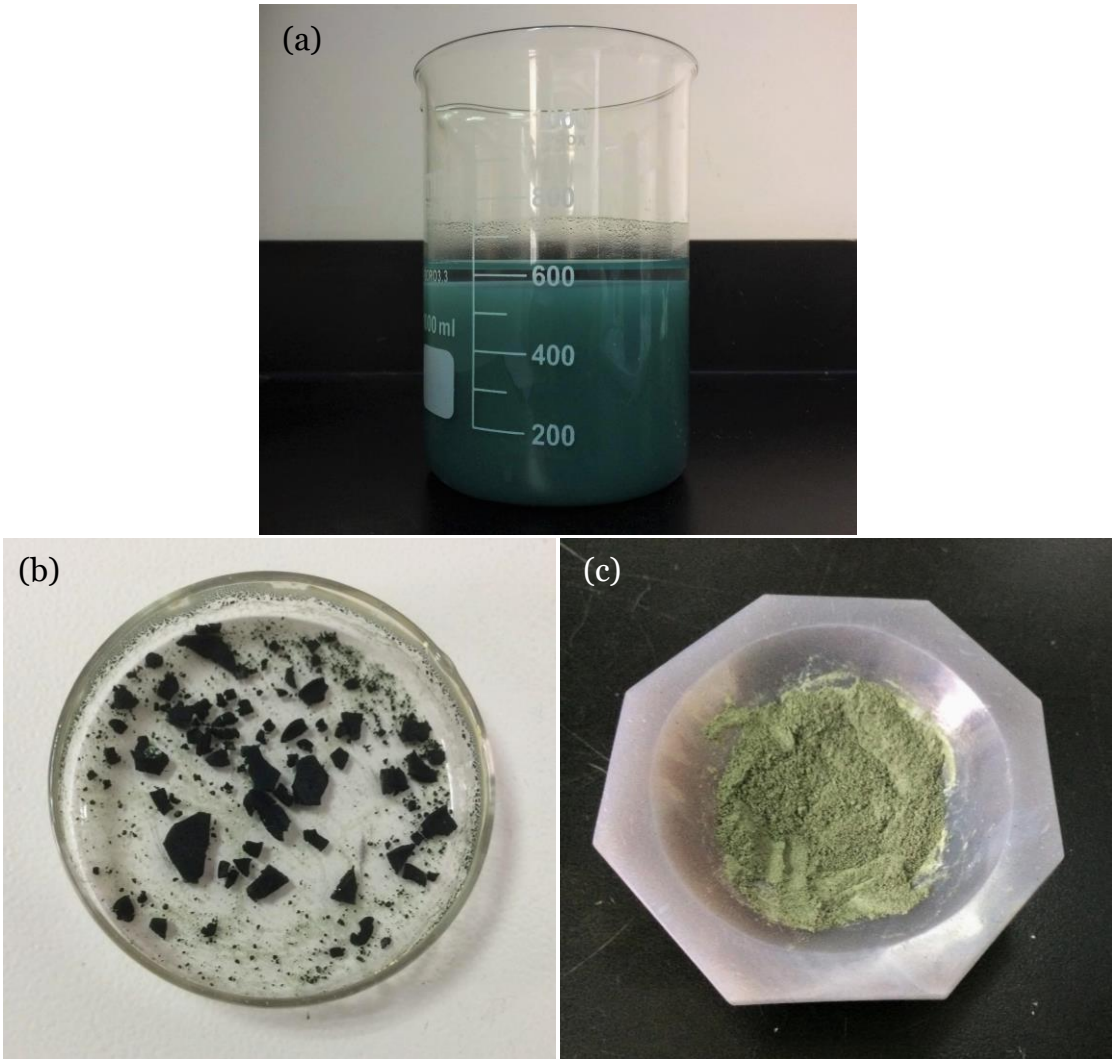

Figure 8: Steps in the process of hydrothermal synthesis of LaCrO3 nanoparticles (a) Precursor lanthanum chromite gel with a clear separation from the water (b) The precipitate after drying in the oven (c) The milled powders before sintering

2.2 Sintering

The sintering of the powders was conducted in a muffle furnace. The powders were first poured into a tungsten carbide die and pressed by hand, see Figure 8 (c). The green compacts were then heated at a constant rate of 8 ˚C/min up to 1400 ˚C and held for 5 hours before cooling down. In previous work the density of the microstructure increased with an increasing sintering temperature up to 1400 ˚C. After this point the relative density started to decrease with an increased temperature, which can be associated with the decomposition of lanthanum chromite solid solution and loss of Cr (81).

2.3 Electrochemical Testing

To evaluate the electrochemical performance of the catalyst a galvanic cell was constructed with the catalyst material as the WE. The catalyst ink was prepared by mixing 5 mg of catalyst powder, 655 µL of ethanol and 20µL of Nafion solution (5wt%) with 326 µL of deionized water in a tube. The tube was put into an ultrasonic cleaning machine for 45min, until the solution had been resolved. Carbon papers were cut into pieces of 1x1.7cm and cleaned in ethanol and by an ultrasonic cleaning machine for 30min. After being dried in air the paper was

connected to an electrode and a surface of 1x1cm was exposed to the electrolyte solution. 20 μL of the catalyst solution was distributed on the paper and dried at room temperature. The catalyst loading was 0.1 mg cm^{-2}.

The electrochemical experiments were performed under ambient conditions in a H-type electrocatalytic cell, separated by a Nafion 211 membrane. The anodic and cathodic compartments were held separated to restrict diffusion of NH_3 to the anode with only H^+ transmission. An Ag/AgCl electrode saturated in KCl was used as the reference electrode and a graphite rod as the counter electrode. A sodium sulfate solution (Na_2SO_4) was used as electrolyte, with a volume of 35ml and a concentration of 0.1M. The setup used in the experiment is presented in Figure 9, argon was used as an inert gas.

The synthesis was performed with N_2 gas is supplied to the cathode chamber. The primary reaction at the anodic compartment is the oxidation of H_2O to produce O_2 and H^+. The protons are transported through the membrane to the cathode where it reacts with the N_2 dissolved in the electrolyte solution and produce NH_3 (14).

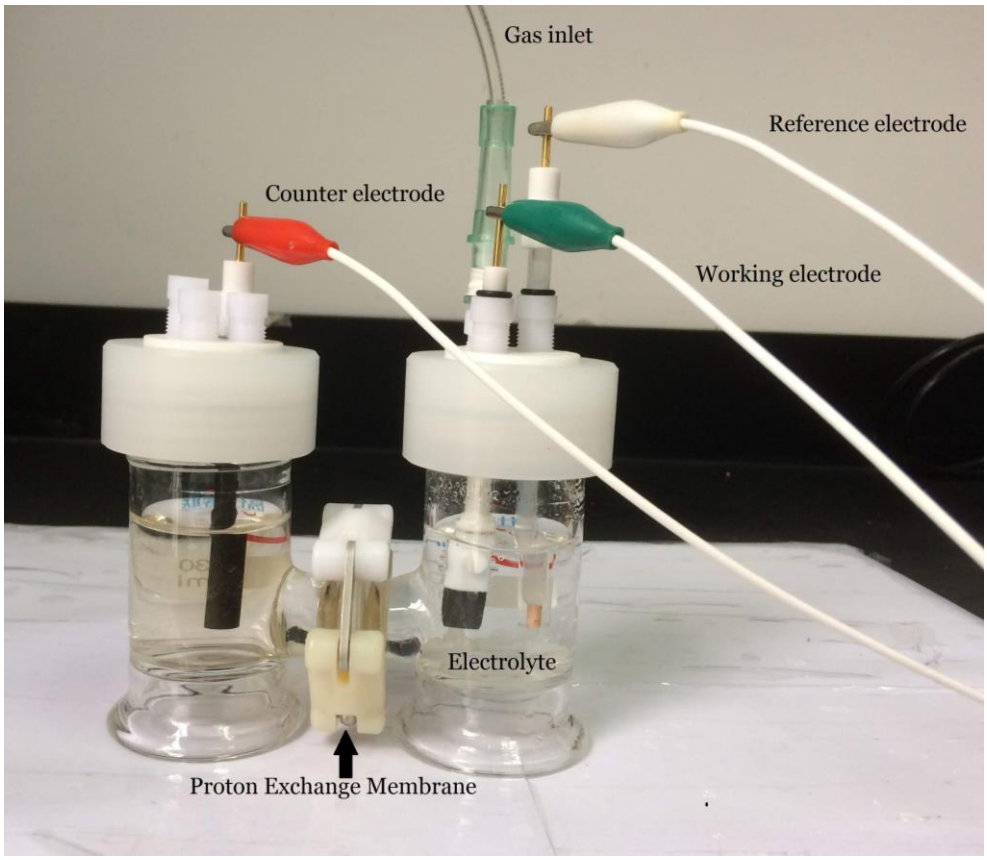

Figure 9: H-type electrolytic cell used for electrochemical testing.

All overpotentials are reported on the RHE scale. The measured potentials vs. Ag/AgCl can be converted to the RHE scale according to the Nernst equation by (94) (95):

$$E_{RHE} = E_{Ag/AgCl} + 0.059\,pH + 0.197 \quad (16)$$

In 0.1M Na_2SO_4 the pH=7 which gives:

$$E_{RHE} = E_{Ag/AgCl} + 0.61 \text{ [V vs. RHE]} \quad (17)$$

Primarily a comparison study was conducted with linear sweep voltammetry. An LSV curve was plotted with Ar gas bubbling into the solution and a sensitivity of 1.e-002 A/V. The gas was then changed to nitrogen for the electrochemical synthesis of ammonia. When the solution was saturated another LSV curve was recorded to qualitatively distinguish the best potentials for the synthesis. The LSV curve (see Figure 11) showed a distinct current enhancement between -0.8 and -0.9 V vs. RHE. When moving towards more negative potentials the favourable current for N_2 is dispersed. This indicates that the competing reaction HER increases and that adsorbed H atoms are taking over on the catalyst surface.

The amperometric tests were then performed at five different potentials: -0.6, -0.7, -0.8, -0.9 and -1 V vs. RHE.

2.4 Ammonia Determination

To determine the ammonia yield for the different potentials the salicylate method and spectrophotometry were conducted. The method is developed from the indophenol blue method but with Sodium Salicylate as the colour developing agent (85). The final solution contains together with the sample solution an oxidizing agent (OA), a colour developing agent (CDA) and a catalyst agent (CA). See Table 2 for the chemicals used.

Table 2: The chemicals used in the Salicylate method.

Chemical	*Molar mass [g mol^{-1}]*	*Mass [g]*
$C_7H_5NaO_3$	160.11	6.40
NaOH	40	1.28
NaClO (5.5%)	74.44 (ρCl≈4-4.9kg/m^3)	7.9ml
NaOH	40	0.30
$Na_2(Fe(CN)_5NO)H_2O$	297.95	0.10

The solutions were prepared as follows:
OA: A sodium hypochlorite solution 14.5% consisting of NaClO (5.5%) and Sodium hydroxide (NaOH) were mixed with deionized water to a volume of 10ml. The solution is sensitive to light, so it was stored cool and dark
CDA: Sodium salicylate ($C_7H_5NaO_3$) and NaOH were mixed in a tube and dissolved when adding deionized water to the level of 100ml.
CA: Sodium nitroprusside dihydrate $Na_2(Fe(CN)_5NO)H_2O$ was dissolved in deionized water added in the amount for a resulting solution of 9.4ml.

The mixing procedure was then preformed with the different solutions added in steps and mixed properly in between. At first 4ml of the sample solution and 50µl of OA were added and mixed following 500 µl of CDA and 50 µl of CA. After 60 min away from light the final solution was then spectrophotometrically tested, and the UV-Vis absorbance spectra recorded at a wavelength of 655nm for ammonia evaluation.
A standard curve was constructed to get the relationship between the absorbance spectra and the concentration of ammonia. 6 samples with known

concentrations of ammonia chloride were matched with their absorbance spectra, see Figure 10. The obtained calibration curve fitted to the points was y=0.54357x+0.044 and is presented in the results in Figure 12.

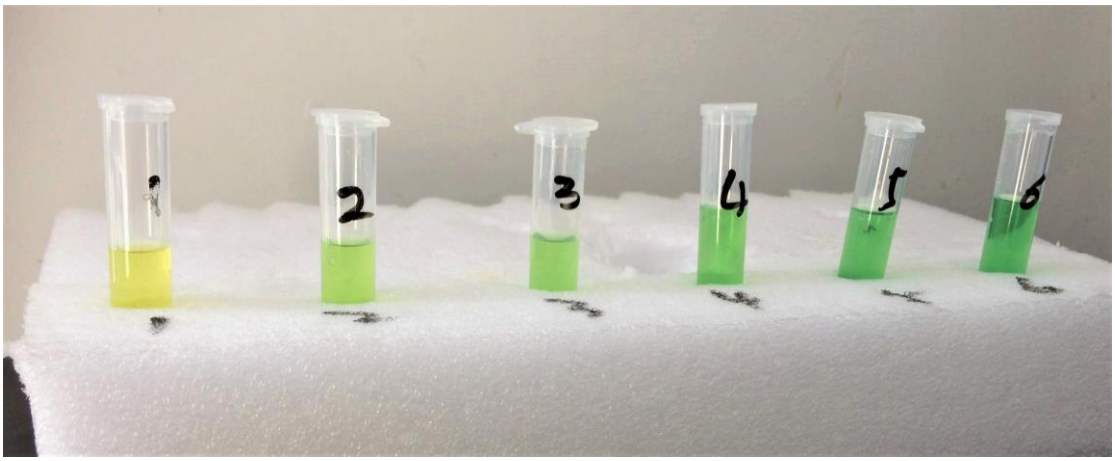

Figure 10: Calibration curve for colorimetric NH_3 evaluation using the Salicylate method

Applying the Beer's Law which states the linear relationship between the absorbance and the concentration of a sample, the ammonia formation rate can then be calculated through Equation 18 (83).

$$Ammonia\ yield\ rate = \frac{C_{NH_3} \times V}{t \times m_{cat}} \tag{18}$$

with:

C_{NH_3}	the measured concentration of ammonia	[µg ml^{-1}]
V	the volume of the solution for ammonia collection	[ml]
t	the time of electrochemical reaction	[h]
m_{cat}	the mass of the working electrode	[mg]

Faraday's Law calculates the algebraic variation of the amount of substance of species *i* during the time interval Δt (96). The Faradic Efficiency (FE) represents the fraction of the actual current used for the half-reaction in question. It's the ratio between the variation of the amount of a given species in the medium used and the corresponding variation that should be expected from Faraday's Law if the totality of the current was used for the half-reaction to progress. See Equation 19.

$$FE = \frac{\Delta n^{effective}}{\Delta n^{F}} = \frac{\frac{C_{NH_3} V}{M_{NH_3}}}{\frac{v_i}{v_e F} Q^F} = \frac{C_{NH_3} V v_e F}{Q^F M_{NH_3} v_i} \tag{19}$$

with:

v_i	the algebraic stoichiometric number of species i	
v_e	the algebraic stoichiometric number of the electron	
F	the Faraday constant	[C mol^{-1}]
Q^F	The quantity of applied charge	[C]
M_{NH_3}	The molar mass	[g mol^{-1}]

Assuming three electrons were needed to produce one mole of NH_3 we have v_i =+1 and v_e =-3 and the FE could be calculated. This gives an important parameter to calculate and compare the efficiency for the catalyst in the electrochemical NRR.

The result of this report is divided into two parts where firstly, the amperometric tests are presented and secondly, the characterisation and analysis of the particle structure and composition.

1 Electrochemical Testing

Figure 13 shows the amperometric i-t curves for 5 different potentials in N_2 saturated 0.1 M Na_2SO_4. The time for the electrochemical reaction was 2 hours with the applied overpotential as well as 15 min gas infusion before starting the test for the electrolyte to get saturated. The current density shows the activity of the reduction process in the electrochemical system. It shows an increased current with increased potential. To evaluate the selectivity and distinguish the NRR from the HER the solutions at the cathode were collected after every performed potential.

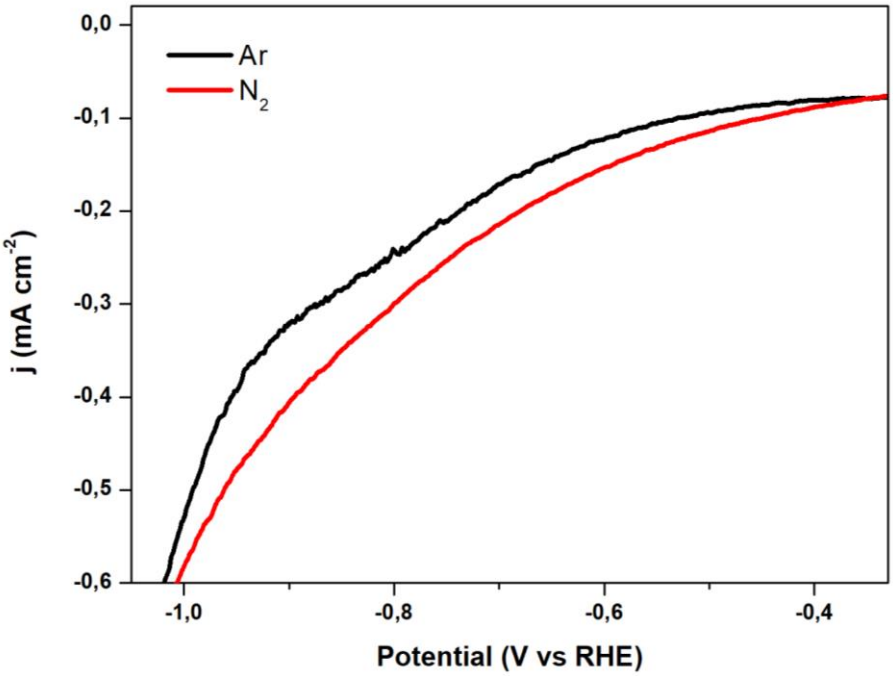

Figure 11: LSV curve of $LaCrO_3$ in Ar- and N_2-saturated 0.1 M Na_2SO_4

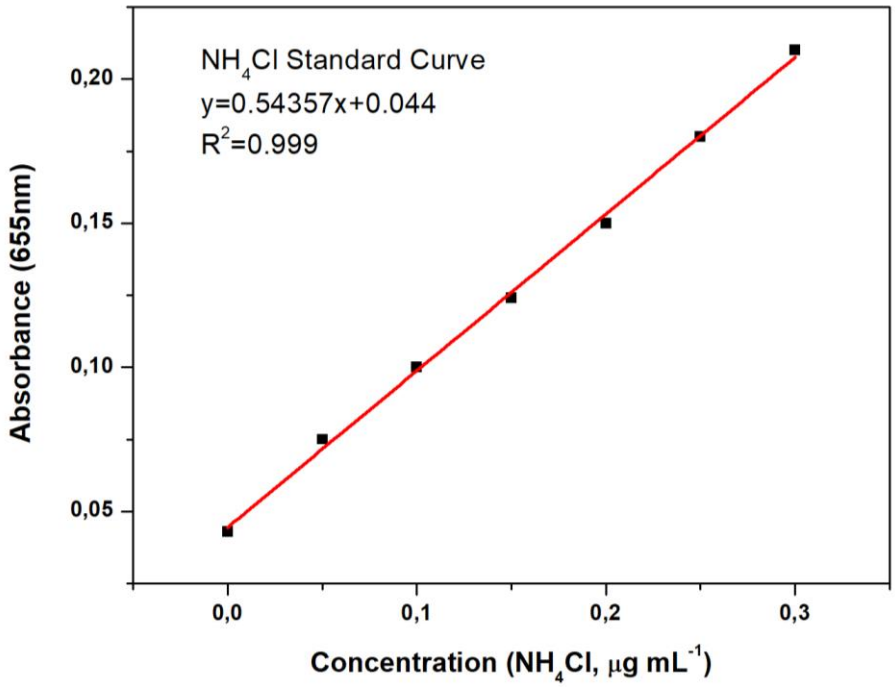

Figure 12: Calibration curve for colorimetric NH_3 evaluation using the Salicylate method

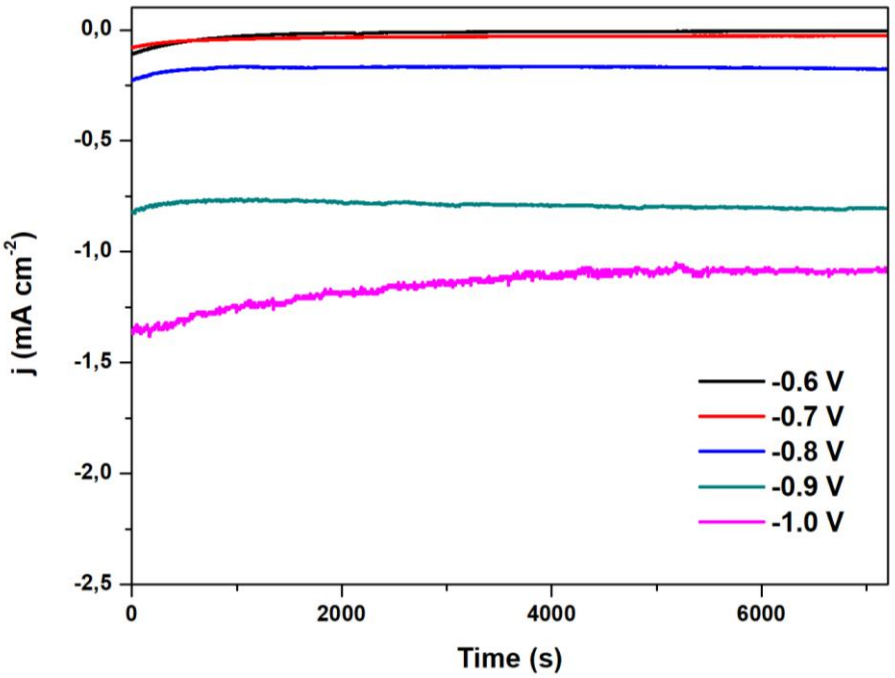

Figure 13: Current density curves over $LaCrO_3$ at different potentials

Additionally, the UV-Vis spectra of the electrolyte solutions collected from the cathode cell is represented in Figure 14. The highest absorption was observed in the solution at an applied potential of -0.8 V vs. RHE. The curves were obtained by using the salicylate method to color the solutions and thereafter measure the absorbance in a spectrophotometer. The results were compared to a calibrated curve (Figure 12) with known concentration of ammonia to get the concentration.

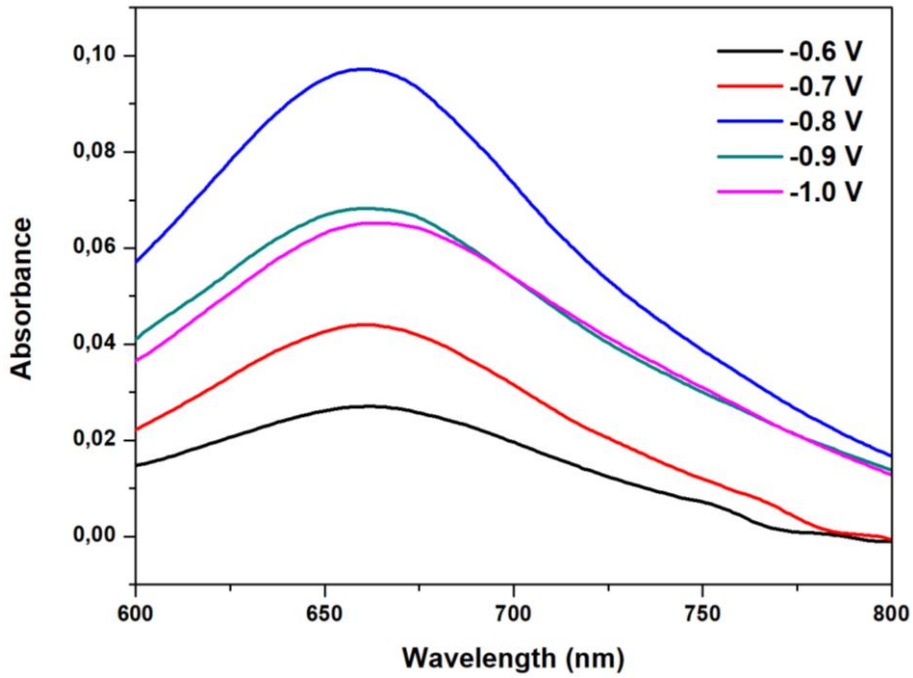

Figure 14: UV-Vis absorption spectra

Figure 15 confirms that the best ammonia yield was obtained at -0.8 V vs. RHE with an ammonia formation rate of 24.8 μg h^{-1} mg^{-1}_{cat}, As well as the best FE of 15%. The same test was repeated at 3 different times and the average result is represented in Figure 16, with a maximum ammonia formation rate of 18,5 μg h^{-1} mg^{-1}_{cat}, as well as an FE of 7.4%.

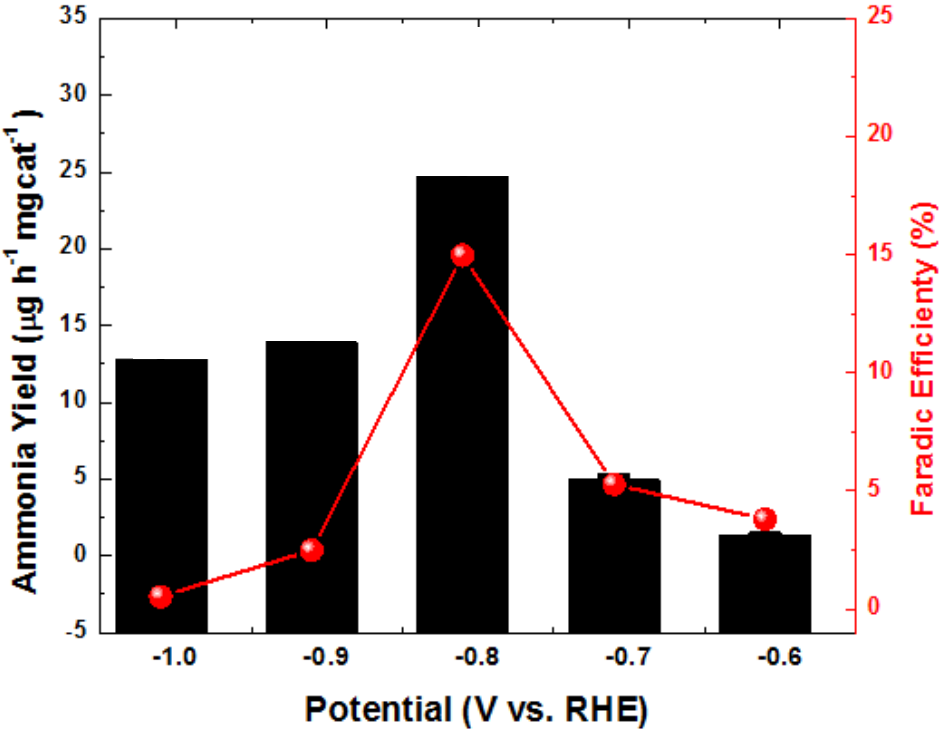

Figure 15: The best NH3 yield and FE for electrochemical NRR over LaCrO3 under corresponding potentials during 2h

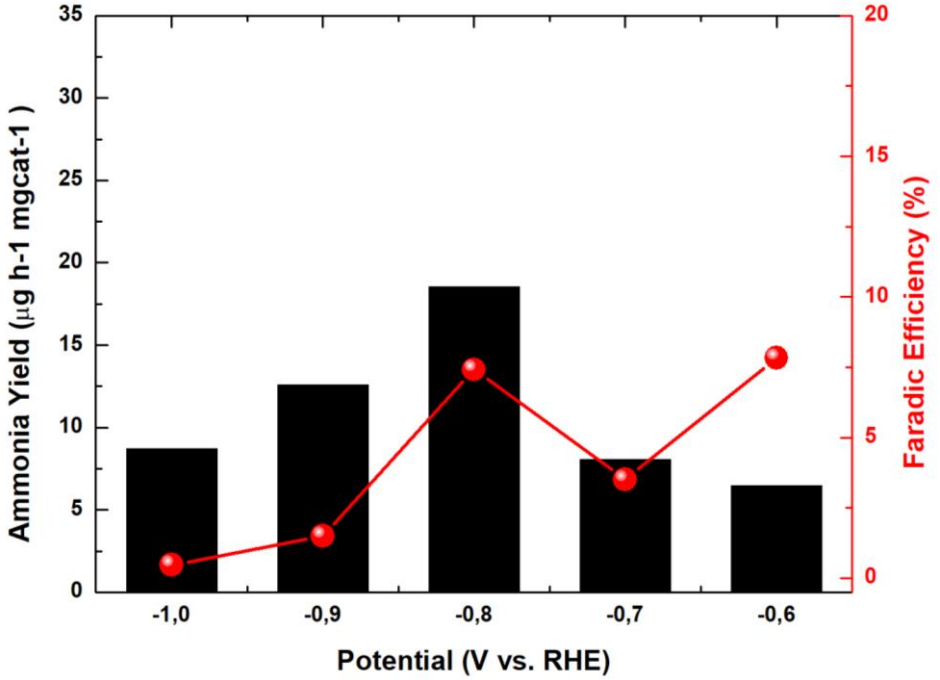

Figure 16: The average result (from 3 repeated tests) of NH_3 yield and FE for electrochemical NRR over $LaCrO_3$ under corresponding potentials during 2h

This is a good result when comparing it to other electrocatalysts under similar conditions, see Table A. 1. Compared to a La_2O_3 nanoplate prepared by Xu et al. with a NH_3 formation rate of 17.04$\mu g h^{-1} mg_{cat}^{-1}$ and a FE 4.76% (97), our result is a great improvement. Two papers were found where a greater NH_3 yield was achieved, this for nanostructured Cr_2O_3 (98) and MoO_3 (99). This will be further discussed in the discussion part.

The stability of the catalyst was then tested as it's another important parameter for the performance and the catalyst showed a stable performance for 24h, Figure 17.

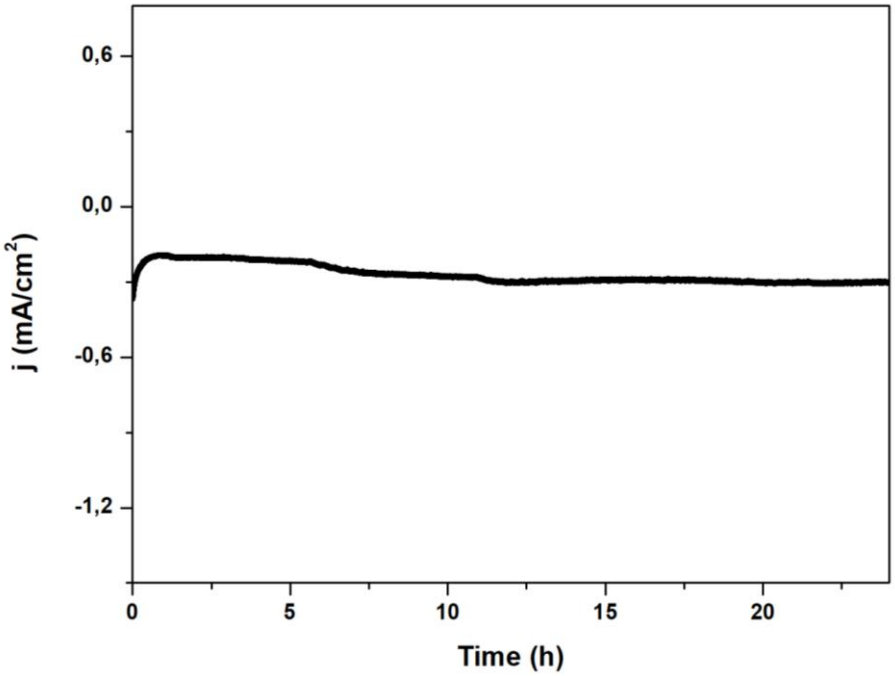

Figure 17: Time-dependent current density curve for $LaCrO_3$ at -0.8V for 24h

2 Analysis of Particle Composition and Structure

2.1 X-Ray Diffraction Analysis

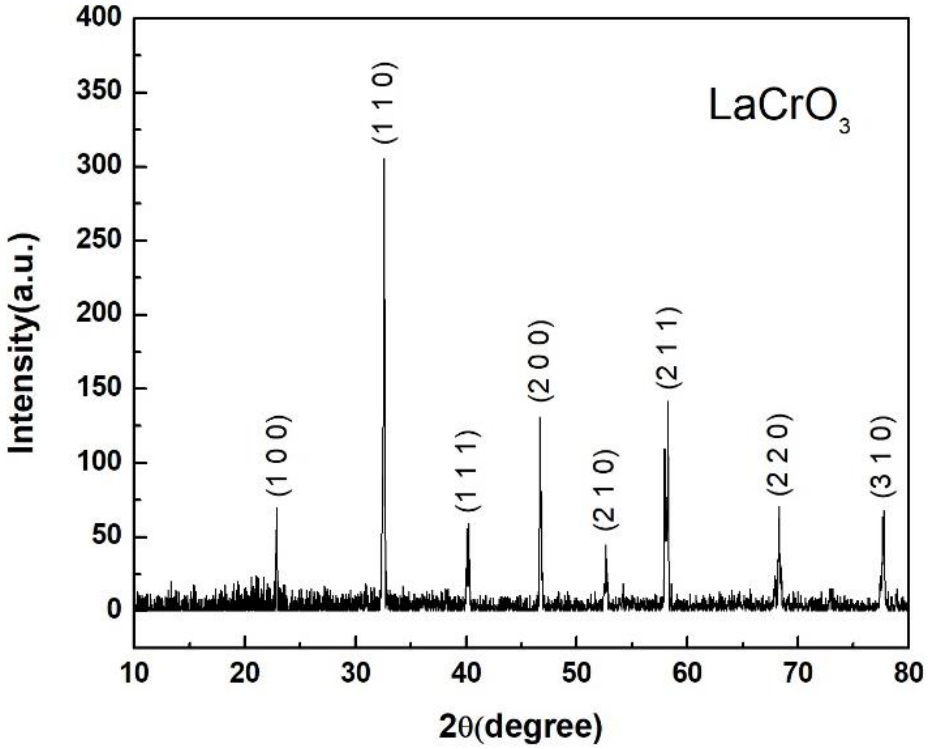

Figure 18: X-Ray Powder diffraction pattern of LaCrO3 processed in NaOH at 200˚C for 20h.

To determine the crystalline phases and the lattice parameter constants for the produced $LaCrO_3$ powders an XRD analysis was performed. The pattern is showed in Figure 18 with an X-ray diffraction with 2˚ beam incidence. The intensity is measured in arbitrary unit. The peaks are sharp which shows that the crystals were formed accordingly with a high degree of crystallinity. The smooth baseline indicates a high purity of the as-prepared samples, with no presence of secondary phases. All the diffraction peaks are aligned precisely with the pattern bulk LaCrO3. The characteristic peaks, corresponding to the (100), (110), (111), (200), (210), (211), (200), (310) planes are recorded at 2θ angles of 23, 33, 40, 47, 53, 58, 69, 78. This corresponds well to standard patterns for the $LaCrO_3$ single phase with orthorhombic *pbnm* structure (100, 101). It confirms the complete transformation of the gel to the perovskite structure (81).

2.2 Transmission Electron Micrographs

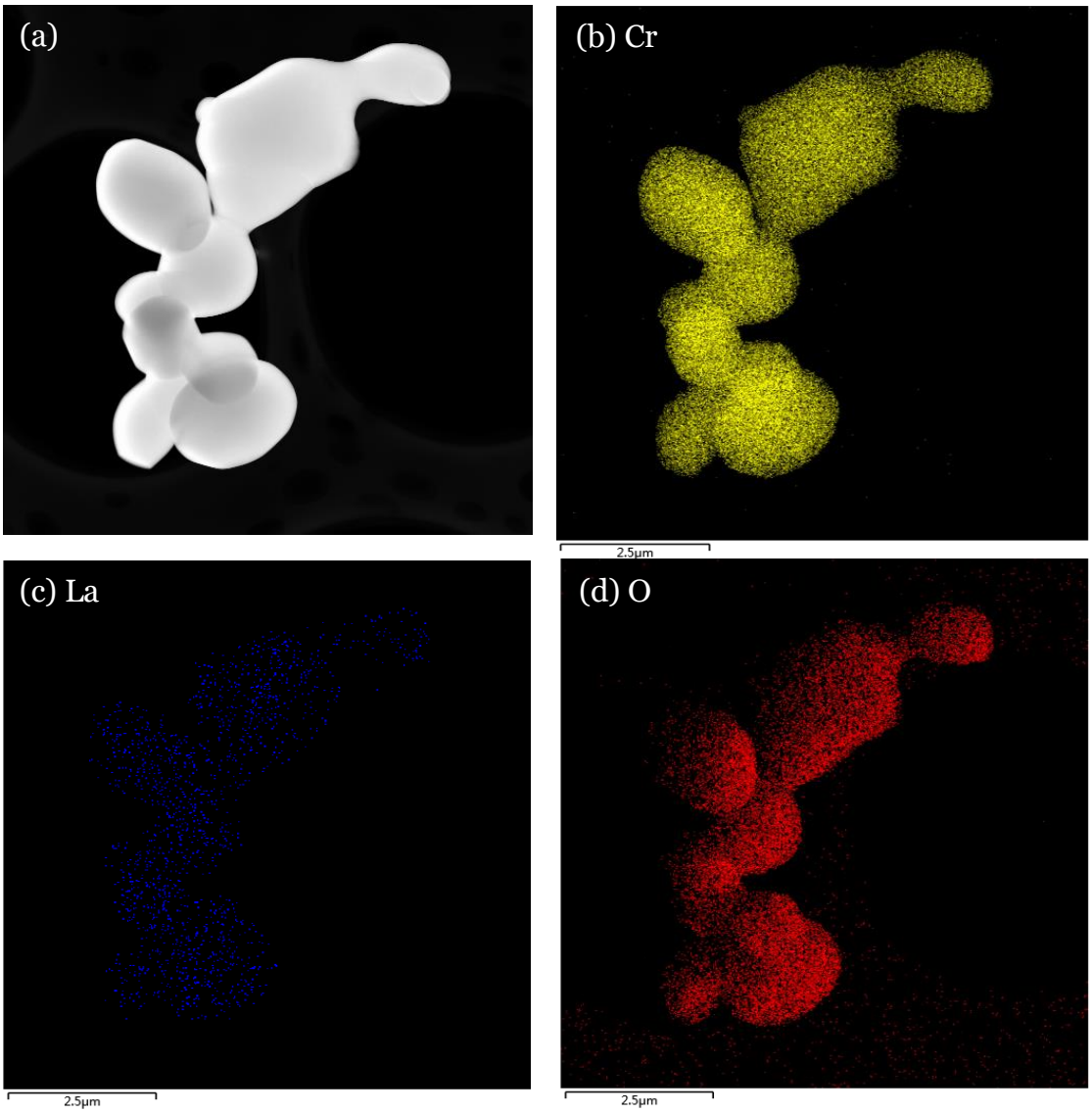

Figure 19: TEM image and elemental mappings of La, Cr and O for $LaCrO_3$ particles

More aspects of the particles were revealed by TEM pictures, see Figure 19. The particles exhibit a regular morphology consisting in platelets, round edges and a homogenous size distribution, the average particle size was ~200nm. Elemental mapping shows a uniform distribution of La, Cr and O elements throughout the particles.

2.3 High Resolution TEM

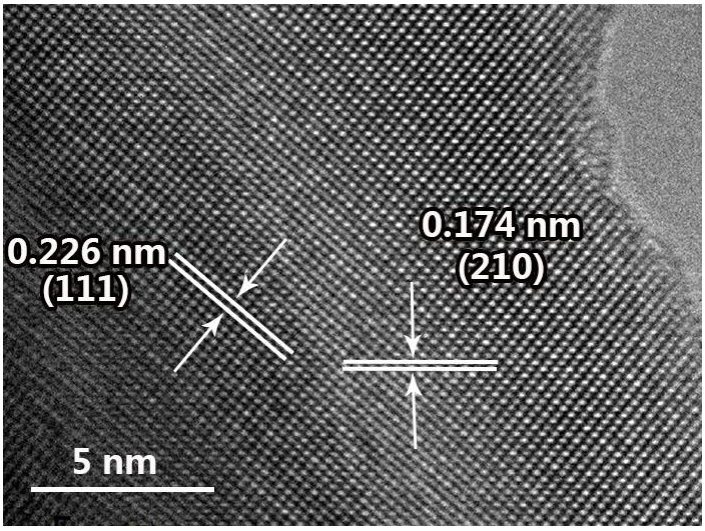

Figure 20: HRTEM image of LaCrO3 particle

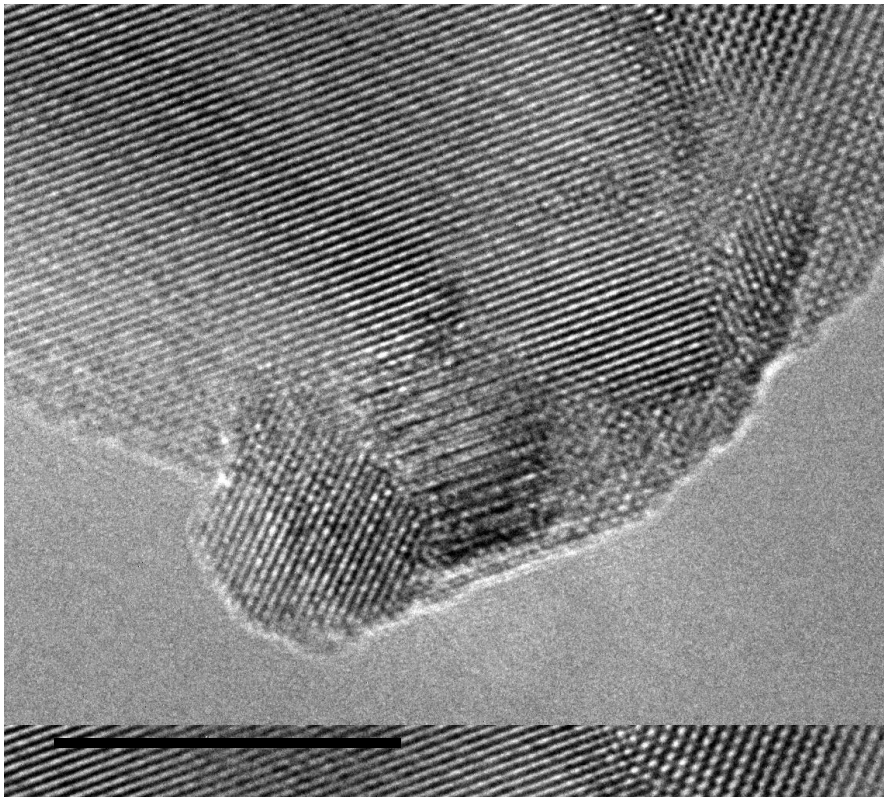
Figure 21: HRTEM image of $LaCrO_3$ particle showing different crystal interactions

The lattice fringes observed in high-resolution TEM image shows a single crystal with a high degree of crystallinity, see Figure 20. The calculated distance 0.226nm spacing is consistent with the (111) planes and the 0.174nm is linked to the (210) plane. Single crystals anisotropic feature shows different physical and chemical properties on various facets in diverse directions. The shapes composed on different crystal facets such as surface atomic arrangement and coordination will highly effect the surface properties (80). The unit cell volume and its parameters are all related to the radii of the A-site ion in the perovskite ABO_3 structure (78).

Figure 21 shows the edge of a particle with a lower resolution. It pictures different crystals grown together. In the areas that are not single crystalline surface properties will be lost and this should therefore be avoided.

2.4 Scanning Electron Microscopy

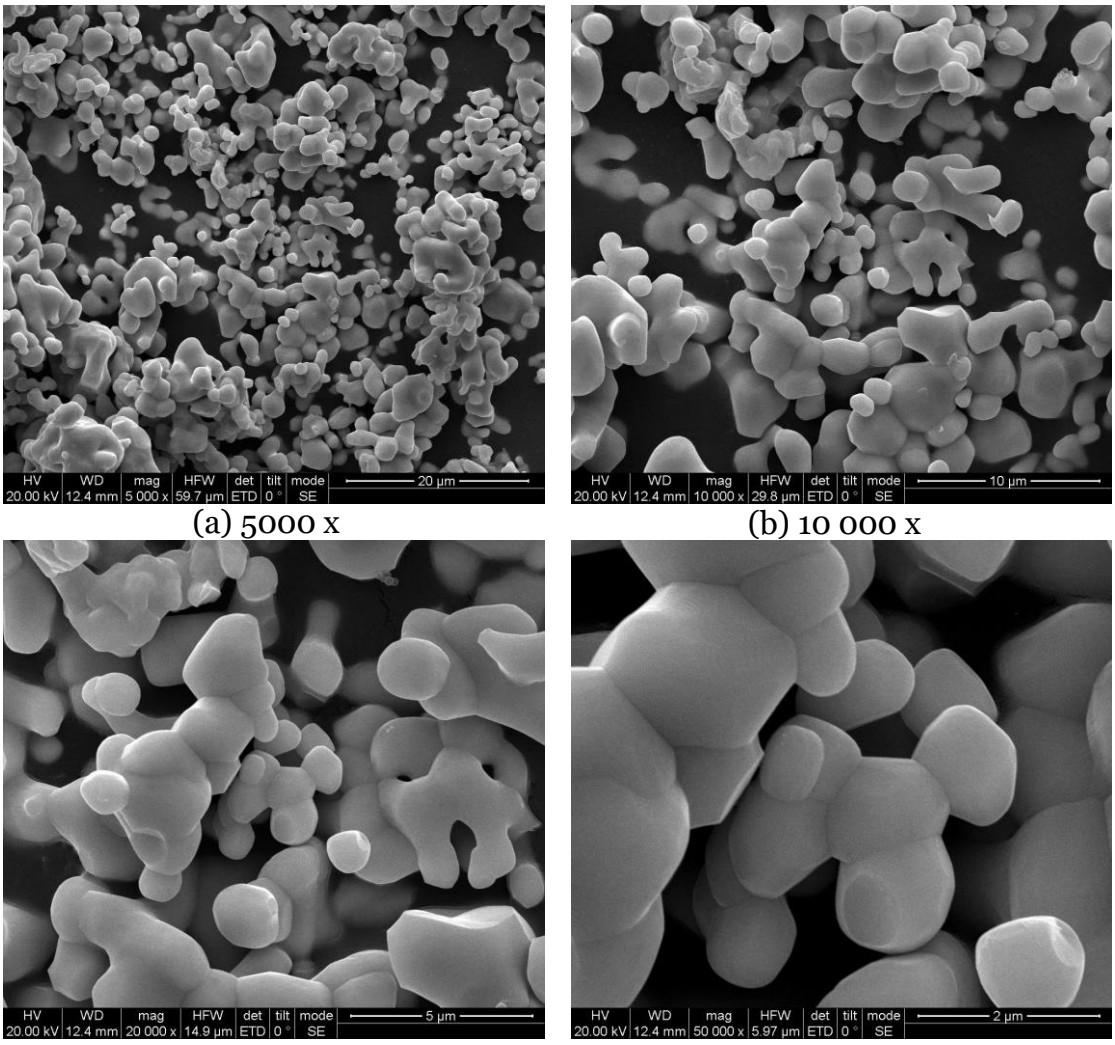

(a) 5000 x (b) 10 000 x

(c) 20 000 x (d) 50 000 x

Figure 22: SEM photograph of $LaCrO_3$

Morphological aspects of the powders were examined by SEM, see Figure 22. For amorphous materials, no clear features or particles can be shown by SEM whereby we can once again confirm our crystalline result. The crystals had a regular shape and particle size and were without any impurity. The small particle size was in the size range of 1-3µm. The agglomeration of the particles is something that should be avoided since this decreases the active surface area.

2.5 Energy Dispersive X-Ray Spectroscopy

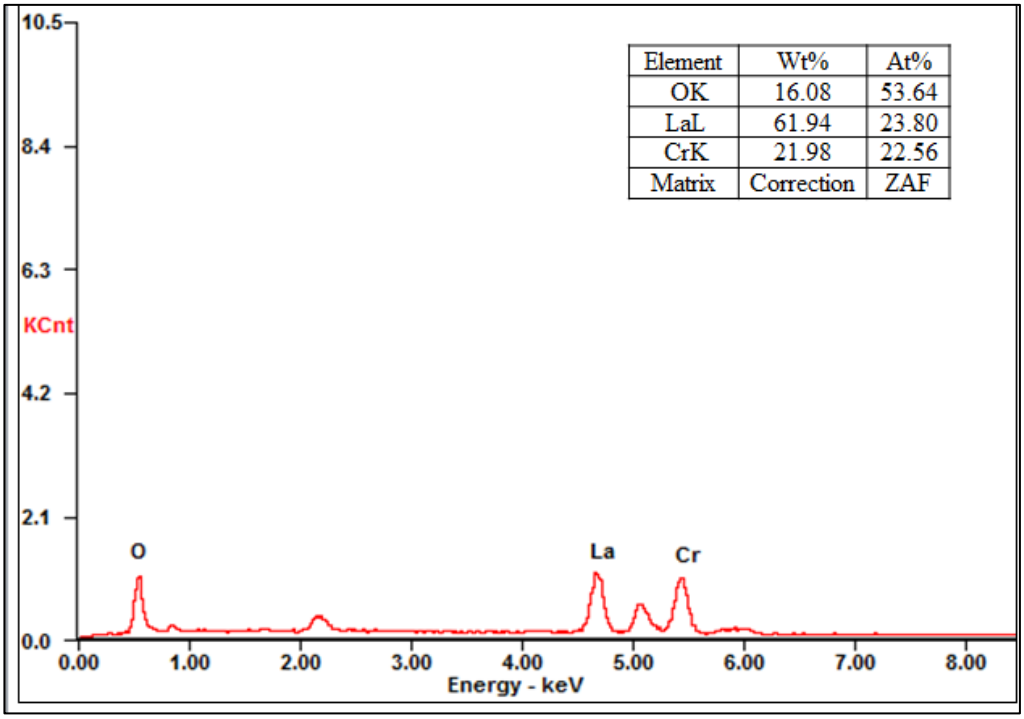

Element	Wt%	At%
OK	16.08	53.64
LaL	61.94	23.80
CrK	21.98	22.56
Matrix	Correction	ZAF

Figure 23: EDS data of LaCrO3 showing the elemental ratios

Energy dispersive X-ray spectroscopy (EDS) gives us a quantitative elemental analysis of our material, see Figure 23. The peaks in the figure represent the atoms in the material and the weight and mol percentage is calculated. Data shows an elemental ratio of the crystals of La:Cr:O=1:1:2 which is close to the ideal perovskite structural composition but with a smaller part of oxygen than expected (78). The deviation from the material stoichiometry with a lower part of oxygen could be the result of some phase impurities.

2.6 X-ray Photoelectron Spectroscopy

An XPS analysis was employed in order to investigate the surface composition and the oxidation states of the as prepared $LaCrO_3$. For all solids, the composition of the surface layer is usually different from the composition of the bulk. This is a useful tool to know in depth the species present at the surface (67). It is especially interesting for the perovskite material because the presence of isolated phases on the surface may strongly influence their surface and catalytic properties (65). $LaCrO_x$ is a complicated system where a number of ternary oxide phases are possible ($LaCrO_4$, $La_2Cr_3O_{12}$, La_2CrO_6 and $LaCrO_3$) depending on the phase composition and temperature during the fabrication process. This can result in the material containing Cr in higher valence states (V or VI) and effecting the catalytic activity (102).

A detailed spectrum was recorded for the following regions: O 1s, La 3d.

2.6.1 O 1s

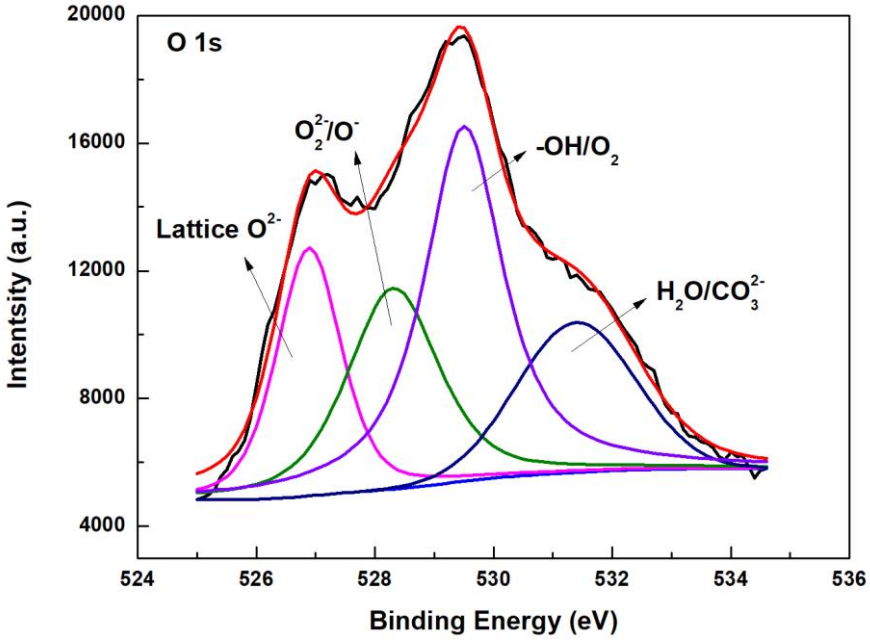

Figure 24: XPS analysis of O 1s spectrum

The nature of the oxygen species on the surface of perovskites can be revealed by an XPS analysis in the O 1s spectrum, see Figure 24. The O 1s spectra shows two major peaks and the absorbed oxygen in the perovskite indicates the appearance of more than one oxygen species. One stronger peak for the O1s spectra at 529.6 eV is related to oxygen in the perovskite structure and indicates that the oxygen ions remain coordinated in structure (103). Different theories explain the origin of these peaks from either different chemical bonds between oxygen-metal atoms, or the defects within the crystal structure (104).

The peak at the lower BE is due to the lattice oxygen O^{2-} (67). While the broad peak at the higher binding energy can be deconvoluting into three distinguished components. The first component has been identified as O_2^{2-}/O^- (67, 105). While that at a higher BE is due to other less electron-rich species of oxygen, such as OH^- or absorbed oxygen (65, 106). The peak at higher BE is assigned to carbonates or molecular water adsorbed on the surface(65).

The less electron-rich oxygen species appearing in the XPS spectrum can be explained by very small amounts of oxides (AO and BO) present at the surface. During the synthesis these components may not have gotten completely incorporated to the perovskite structure. These differences in surface composition could have an effect on both the adsorption and catalytic properties compared to pure perovskites (65).

2.6.2 Cr 2p

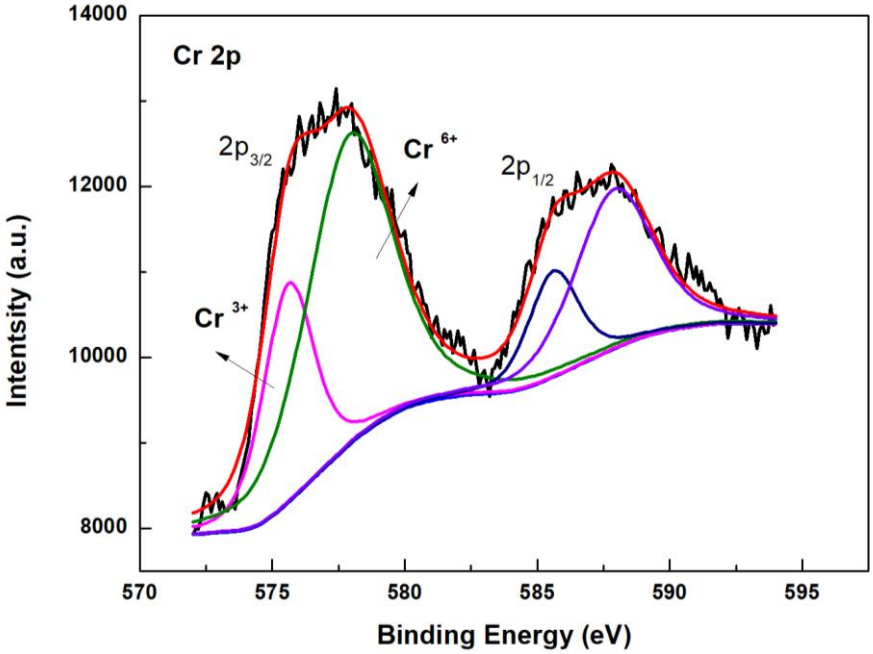

Figure 25: XPS analysis of Cr 2p spectrum

The oxidation state of Cr on the surface of $LaCrO_3$ has been studied in Figure 25. The result is two large peak levels ($2p_{1/2}$, $2p_{3/2}$) and its deconvolutions. The result confirms Cr from other studies as well as the presence of oxidised phases (107). The peaks at BE 575 and 577 correlates to Cr with a mixed oxidation states of 3+ and 6+ (104). The surface concentration of the transition metal ions on the perovskite is of certain interest for their role in the catalytic activity. The specific oxidation state has in other studies been recognized as an important parameter for the catalysis (108).

2.6.3 La 3d

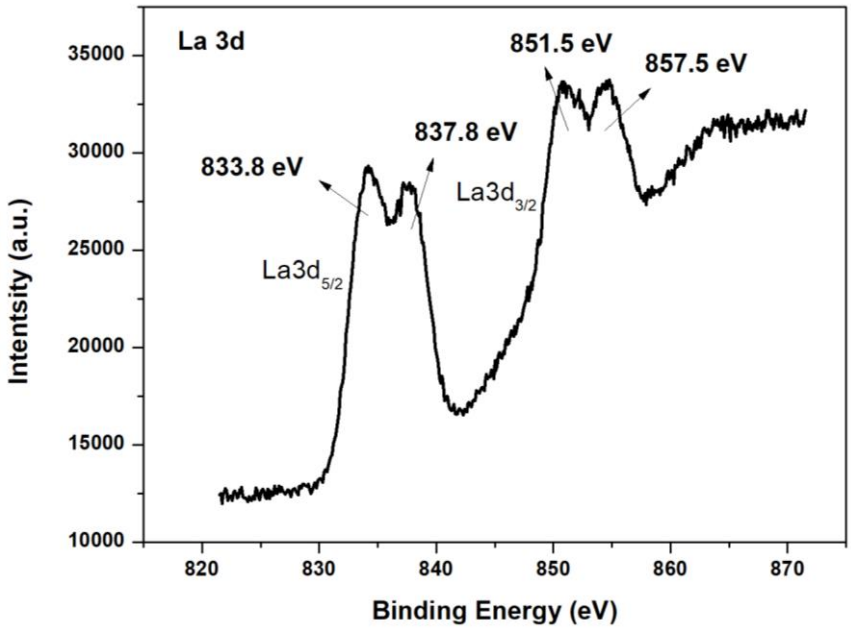

Figure 26: XPS analysis of La 3d spectrum

Lanthanum is the perovskite structure support and the oxidation state can have an effect of the reaction pathway during NRR, as well as affecting the oxidation state of the B cation. XPS analysis in the La 3d spectrum (Figure 26) verifies the lanthanum from the strength of the BE and the intensity with two main peaks at around 835.8 and 852.58eV (107). The two peaks are further split by multiple splitting as a result of contributions from several initial and final states (109, 110). The valence state of La^{3+} is confirmed consistent with the La $3d_{5/2}$ BE (100). At the higher BE an alternative binding energy than that of the perfect perovskite is showed. The peaks can be associated with La_2O_3 or $La(OH)_3$, resulting from La surface segregation (49, 100).

Discussion

1 Experimental Results

Perovskite $LaCrO_3$ was successfully synthesised by the hydrothermal method. The result was a highly crystalline material as showed by the XRD and the crystal facets could be determined. The plane phase orientation plays an important role in catalysis where some planes contain more active sites and the particles can be tailored from that information. The final result was orthorhombic *pbnm* $LaCrO_3$ particles, confirmed by the results in other studies.

With the material production process involving only one-step hydrothermal reaction it was confirmed as an easy and economical production process. The particles obtained a small size in the scale of 200nm and a size distribution with little variation. The particles show some agglomeration as pictured by the SEM which will decrease the active surface area. An extended milling process could therefore have been favourable. The milling in this experiment was performed by hand which leads to a difficulty in keeping control over pressure and a uniform result. Another factor promoting the uniform and mono-disperse growing of particles is mild synthesis conditions. The heat treatment in this study of 200˚C for 20h was an adaption between the available properties of the furnace and the result presented in other studies. There are two competing characteristics when choosing the temperature and the interval for the process in the hydrothermal synthesis. It's the goal of a high crystalline material with a good growth and recrystallization speed of $LaCrO_3$ crystals, that's increased with increased temperature. But also, the formation of uniform and mono-disperse particles which will be better at milder conditions. To ensure the best result for the $LaCrO_3$ production in this process different heat treatments would have been needed and compared to find the optimal conditions.

The HRTEM shows a single crystal with the planes (111) and (210) projected, with a high degree of crystallinity. The disadvantage with the high-resolution image is that it can only focus on a small part at a time. It was also restrained to only the very thinnest areas of the particles for a picture to be possible. An overall conclusion of the crystal growth in the whole particles can therefore not be concluded from these pictures. Although the XRD result confirms a single-phase crystalline material. Edges with several crystal phases as well as the interaction of two larger crystals is also seen in the HRTEM. A high crystallinity is the aim for the catalyst in NRR as it facilitates mass transfer and increases the active surface area.

The surface composition of the transition metal ions is another very interesting property, crucial for the catalytic activity. In the XPS of the Cr 2p region, Cr with a mixed oxidation state of 3+ and 6+ was identified. This together with the great result of ammonia yield and FE proves that Cr^{3+} and Cr^{6+} are efficient catalyst ions for the nitrogen reduction. The perovskite structure offers a great flexibility in oxidations states of its cations and further optimizations of the composition

to boost NRR is of great interest. The oxidation state of the A cation (La) will also highly affect the oxidation state of the B-site cation and might cause structural defects such as vacancies. This is another favorable property that can be tailored for the NRR.

The EDS indicates some form of impurities since the stoichiometry does not match the perovskite $LaCrO_3$ structure. This has probably occurred in the fabrication process and might be the result of some unwanted phases in the material. Previously discussed $La(OH)_3$ could be a result of high temperature reaction conditions, where the solubility of this molecule will be increased. The alkalinity of the solution will also affect the outcome of the synthesis and this should be further investigated. The $La(OH)_3$ might also be present on the surface, concluded from the XPS in the La 3d region. This might affect the adsorption and activation of nitrogen.

The amperometric test demonstrated an efficient NRR compared to the competing HER over an $LaCrO_3$ at an applied overpotential of -0.8 V vs. RHE. When increasing the potential more, the reaction kinetics of the hydrogen started to take over on the catalysts surface and the FE decreased. The average NH_3 formation rate of 18,5 $\mu g\ h^{-1}\ mg^{-1}_{cat}$, as well as the average FE of 7.4% shows a good result when comparing to other electrocatalytic NRR with aqueous-based NRR electrocatalysts. It shows a great improvement from the lanthanum oxide (La_2O_3) nanoplate (NH_3 17.04$\mu g h^{-1} mg_{cat}^{-1}$ FE 4.76%) (97). This confirms the role of Cr as an active transition metal catalyst in NRR, as well as the advantage of the perovskite structure. Compared to other oxides the perovskite shows a great FE as well as a high NH_3 yield.

Two previously reported electrocatalysts showed a greater NH_3 yield than $LaCrO_3$. This was achieved when Cr_2O_3 (98) and MoO_3 (99) acted as the catalyst, under similar conditions as in this experiment. They were both hydrothermally produced, but one main difference was in their nanostructure. The MoO_3 was produced as flake-like nanosheets and the Cr_2O_3 had a multishelled hollow structure. This could be one advantage of these catalysts as it can provide more active sites as well as better mass transfer for the reactants over the catalyst.

One big challenge with the experiment was the stability in the electrochemical setup. The result during the tests were stable, as confirmed by the 24 h stability test. But when reusing the catalyst several times for a recycle test, a continuity in the result was not successfully achieved. This indicated that the system was very sensitive to small changes in the setup as the result at one test got worse to then the next time show a better activity again. With the limited amount of time this phenomenon could not be further investigated. It can for example have been due to pollution of ammonia in the cell when changing the electrolyte, an unstable performance of the membrane separating the cells, diffusion in between the chambers or that the catalyst material not was stable and changed its structure.

I also intended to do a study with $LaCrO_3$ in a different electrolyte to see if the FE would increase. As this had been reported by others with potassium sulfate (K_2SO_4). After several attempts this was though stopped since the performance

showed a completely unstable result where no performance peak could be attained. This also confirms the stability problem in the setup and that K_2SO_4 might not be applicable with $LaCrO_3$.

2 Source of Error

The stability of the experimental setup was a problem. When evaluating the NRR vs. HER with the linear sweep voltammetry the result with the inert argon gas sometimes showed a higher activity then when nitrogen gas was applied. It was also better to not have the gas at all compared to add nitrogen gas. Since this only was a comparison study and did not have an effect on the final result it was not further investigated, but this continued to be a challenge also in the amperometric tests. A graph of the average performance of the catalyst was also presented in the result to support the graph of the best ammonia yield and FE. This showed a lower result and a different shape of the curves. To strengthen the result of the performance more tests might have been needed. Both to if possible, increase the average values, as well as to further understand the parameters affecting the stability of the system.

In the experimental setup one parameter that could have an effect for the result was the gas flowrate of the nitrogen. This parameter was hard to control due to rough calibration equipment. The optimal flow rate for NRR or if it, as concluded by some other papers was rate independent, was not investigated in this experiment.

The absorbance measurements also showed different results when performing the ammonia determination and the salicylate method. Since the tests were performed several times during a longer period, the neutral electrolyte solution was always measured as a reference. The absorbance result of this solution usually differed between the different test round. This could be adjusted in the calibration curve, but the source of error was not identified.

It was also not eliminated the possibility that the detected reduction products were generated from other reactions than via the NRR. To eliminate produced ammonia at an open circuit potential or by an Ar saturated electrolyte would have made the result more reliable.

Another possible phenomenon is the crossover of produced ammonia back to the anode, where it oxidizes. Collecting the solution also from the anode chamber and measuring the ammonia concentration in that electrolyte would have given additional information if this unwanted membrane crossover occurred.

Conclusion and Further Research

In summary, Lanthanum Chromite ($LaCrO_3$) nanoparticles were synthesized and evaluated as NRR electrocatalysts in an aqueous based cell under ambient conditions. The particles had a homogenous size distribution with an average particle size of 200nm and round edges. The particles obtained a high crystallinity and the transition metal Cr contained a mixed oxidation state of 3+ and 6+ at the catalyst surface. The best ammonia yield was obtained at -0.8 V with an ammonia formation rate of 24.8 $\mu g\ h^{-1}\ mg^{-1}_{cat}$, and Faradic efficiency of 15%. The catalyst also showed a good stability. The NRR activity is great compared to other oxide and noble metal catalysts with a particularly good FE. These results show a promising direction for further catalyst optimization in the field of perovskite structured electrocatalysts for NRR.

The doping of perovskite structured catalysts has shown a great performance improvement in other reduction processes. By doping additional compounds can be introduced to boost the active area for the NRR. With partial substitution of ions in the structure vacancies can also be introduced. This can for example occur by incorporating ions with a different radius in the lattice.

Recent attention has also been drawn to the electrolyte in the electrochemical process and particularly its possible role in suppressing the competing HER. By choosing an electrolyte that to a lesser extent provide protons to the catalysts surface, FE has been showed to increase.

With the goal of a commercial process for an economical and environmentally sustainable ammonia synthesis many more requirements need to be fulfilled. The field of electrochemical ammonia synthesis in ambient conditions is still in an early phase of development. The reported results show many promising directions, but it has only been conducted in the laboratory and in small scale so far. In this study a stability of 24h was proved but this is not enough for an industrial application. To do post reaction analysis would also provide a lot of necessary information for the evaluation of the catalyst's stability during the reduction reaction.

As the research in this field is conducted, the perspective easily gets very narrow. Looking at the nanoscale design is one very interesting focus with a lot of potential, but it must also be put into its context. A perfect catalyst will not be enough if the surrounding environment not is optimized. Different kinds of electrochemical cells are also being researched where different electrolyte are designed and needs to be further developed for the NRR vs. HER reaction.

To continue to develop the theoretical models for the NRR on different catalysts are another important field to get a better picture of the actual possibilities. The necessary applied potential for the current experimental results is still too high compared to the Haber-Bosch process. From the theoretical investigations available today it can also be questioned if it's even possible with a lower energy input for the electrochemical reduction and a satisfying catalytic activity. But,

since the research is young new experimental and theoretical results could provide a new picture. The research for an environmentally friendly way of producing ammonia although have many reasons to be continued. Even if it might not be possible to completely replace the Haber-Bosch process other great benefits can be achieved. The possibility with a small scale, mobile ammonia synthesis method in a completely emission free cycle, is an exciting and much needed technology.

1 Learning and Outcomes

As the topic of this master thesis was a new field to me, of chemistry and catalysis, it has resulted in a lot of new learnings. To do experimental research is a very different way of working compared to theoretical studying. The outcome cannot always be controlled, and many factors will affect the results. I have gained a new understanding for how experimental research faster can provide valuable results, even in cases where the theoretical background is not fully understood. It has also been a big challenge and lesson to perform research on a topic where many new sciences combine and are developed together. To accept that answers doesn't always exist but that your results might still be valuable.

Another great lesson when finishing the paper and getting an overview of the project has been the realization of how many different perspectives that research can be performed from. When other research papers are your source to knowledge you must bear in mind the purpose and angle of those specific papers. This has also been a lesson from the experience of doing experimental research and how the data you gain can be presented in many different ways.

The opportunity to perform the master thesis in a new environment and culture has also been a unique experience. It has improved my ability to cooperate with people of different cultures as well as to overcome language barriers. As the future for renewable energy technology faces a lot of challenges, I believe that the need to cooperate over boarders is crucial. The experiences and friendships I've gained from this project are invaluable and it's something I will cherish and bring with me for the future.

References

1. Capuano L. International Energy Outlook 2018 (IEO2018). U.S. Energy Information Administration; 2018.
2. Nery MCD. One third of global air pollution deaths in Asia Pacific https://www.who.int/westernpacific/news/detail/02-05-2018-one-third-of-global-air-pollution-deaths-in-asia-pacific: World Health Organization; 2018 [Dec 17, 2018]
3. Vittal V. The Impact of Renewable Resources on the Performance and Reliability of the Electricity Grid. The Bridge on Electricity Grid. 2010;40(1).
4. Williams MC. Fuel Cells. In: Shekhawat D, Spivey JJ, Berry DA, editors. Fuel Cells: Technologies for Fuel Processing2011.
5. Valera-Medina A, Xiao H, Owen-Jones M, David WIF, Bowen PJ. Ammonia for power. Progress in Energy and Combustion Science. 2018;69:63-102.
6. Manjunatha R, Schechter A. Electrochemical synthesis of ammonia using ruthenium–platinum alloy at ambient pressure and low temperature. Electrochemistry Communications. 2018;90:96-100.
7. Skulason E, Bligaard T, Gudmundsdottir S, Studt F, Rossmeisl J, Abild-Pedersen F, et al. A theoretical evaluation of possible transition metal electro-catalysts for N2 reduction. Phys Chem Chem Phys. 2012;14(3):1235-45.
8. Kopp Alves A, Bergmann CP, Amorim Berutti F. Introduction. Novel Synthesis and Characterization of Nanostructured Materials2013.
9. Labhasetwar N, Saravanan G, Kumar Megarajan S, Manwar N, Khobragade R, Doggali P, et al. Perovskite-type catalytic materials for environmental applications. Sci Technol Adv Mater. 2015;16(3):036002.
10. Shekhawat D, Berry DA, Spivey JJ. Introduction to Fuel Processing. Fuel Cells: Technologies for Fuel Processing2011. p. 1-9.
11. Alaswad A, Baroutaji A, Achour H, Carton J, Al Makky A, Olabi AG. Developments in fuel cell technologies in the transport sector. International Journal of Hydrogen Energy. 2016;41(37):16499-508.
12. Rees NV. Electrochemistry Fundamentals: Nanomaterials Evaluation and Fuel Cells. In: Ozoemena KI, Chen S, editors. Nanomaterials for Fuel Cell Catalysis2016.
13. Baxter J, Bian Z, Chen G, Danielson D, Dresselhaus MS, Fedorov AG, et al. Nanoscale design to enable the revolution in renewable energy. Energy & Environmental Science. 2009;2(6).
14. Lefrou C, Fabry P, Poignet J-C. Basic notions. Electrochemistry - The Basics, with Examples: Springer; 2012. p. 40-6.
15. Cassidy M, Ouweltjes JP, Dekker N. Going Beyond Hydrogen: Non-hydrogen Fuels, Re-oxidation and Impurity Effects on Solid Oxide Fuel Cell Anodes. In: Lehnert RS-WaW, editor. Innovations in Fuel Cell Technologies. Energy and Environment Series2010. p. 149-89.
16. Turner JA. Sustainable Hydrogen Production. Science. 2004;305(5686):972-4.
17. Paul-Boncour V, Percheron-Guégan A. Introduction to hydrogen storage methods. In: Burzo E, editor. Hydrogen Storage Materials · Hydrogen Storage Materials.

18. Osman O, Sgouridis S. 2018 5th International Conference on Renewable Energy: Generation and Applications (ICREGA). Optimizing the production of ammonia as an energy carrier in the UAE; Al Ain2018.
19. Survey USG. Mineral commodity summaries 2018: U.S. Geological Survey. 2018.
20. Patil BS, Hessel V, Seefeldt LC, Dean DR, Hoffman BM, Cook BJ, et al. Nitrogen Fixation. Ullmann's Encyclopedia of Industrial Chemistry, (Ed)2017.
21. Giddey S, Badwal SPS, Kulkarni A. Review of electrochemical ammonia production technologies and materials. International Journal of Hydrogen Energy. 2013;38(34):14576-94.
22. Kojima Y. A green ammonia economy https://nh3fuelassociation.org/wp-content/uploads/2013/10/nh3fcx-yoshitsugu-kojima.pdf 2013 [Jan 07, 2019]
23. Bomelburg HJ. Use of ammonia in energy-related applications. 1982;1(3):175-80.
24. Zamfirescu C, Dincer I. Ammonia as a green fuel and hydrogen source for vehicular applications. Fuel Processing Technology. 2009;90(5):729-37.
25. Huang K, Goodenough JB. Current, gas flow, utilization, and energy balance in a solid oxide fuel cell (SOFC). Solid oxide fuel cell technology Principles, performance and operations: Woodhead Publishing; 2009.
26. Huang K, Goodenough JB. Thermodynamics of the solid oxide fuel cell (SOFC). Solid oxide fuel cell technology Principles, performance and operations: Woodhead Publishing; 2009.
27. Travis AS. The Synthetic Nitrogen Industry in World War 1, Its Emergence and Expansion: Springer; 2015.
28. Wang K, Smith D, Zheng Y. Electron-driven heterogeneous catalytic synthesis of ammonia: Current states and perspective. Carbon Resources Conversion. 2018;1(1):2-31.
29. Appl M. Ammonia, 2. Production Processes. Ullmann's Encyclopedia of Industrial Chemistry2011.
30. Huazhang L. Ammonia synthesis catalyst 100 years: Practice, enlightenment and challenge. Chinese Journal of Catalysis. 2014;1619–1640(35).
31. Travis AS. The Direct Synthesis of Ammonia. Nitrogen Capture The Growth of an International Industry (1900–1940): Springer; 2018. p. 93-128.
32. Appl M. Ammonia, 1. Introduction. Ullmann's Encyclopedia of Industrial Chemistry, (Ed)2011.
33. Erisman JW, Sutton MA, Galloway J, Klimont Z, Winiwarter W. How a century of ammonia synthesis changed the world. Nature Geoscience. 2008;1:636.
34. Jennings JR. Catalytic Ammonia Synthesis Fundamentals and Practice1991.
35. Hooper CW. Ammonia Synthesis: Commercial Practice. In: Jennings JR, editor. Catalytic Ammonia Synthesis Fundamentals and Practice 1991.
36. Shipman MA, Symes MD. Recent progress towards the electrosynthesis of ammonia from sustainable resources. Catalysis Today. 2017;286:57-68.
37. Hinnemann B, Nørskov JK. Catalysis by Enzymes: The Biological Ammonia Synthesis. Topics in Catalysis. 2006;37(1):55-70.

38. Seefeldt LC, Hoffman BM, Dean DR. Mechanism of Mo-dependent nitrogenase. Annu Rev Biochem. 2009;78:701-22.
39. Wang S, Ichihara F, Pang H, Chen H, Ye J. Nitrogen Fixation Reaction Derived from Nanostructured Catalytic Materials. Advanced Functional Materials. 2018;28(50).
40. Yang D, Chen T, Wang Z. Electrochemical reduction of aqueous nitrogen (N2) at a low overpotential on (110)-oriented Mo nanofilm. Journal of Materials Chemistry A. 2017;5(36):18967-71.
41. Kordali V, Kyriacou G, Lambrou C. Electrochemical synthesis of ammonia at atmospheric pressure and low temperature in a solid polymer electrolyte cell. Chemical Communications. 2000:1673–4.
42. Kugler K, Ohs B, Scholz M, Wessling M. Towards a carbon independent and CO2-free electrochemical membrane process for NH3 synthesis. Phys Chem Chem Phys. 2014;16(13):6129-38.
43. Cui X, Tang C, Zhang Q. A Review of Electrocatalytic Reduction of Dinitrogen to Ammonia under Ambient Conditions. Advanced Energy Materials. 2018;8(22).
44. Matanović I, Garzonc FH, Hensonb NJ. Electro-reduction of nitrogen on molybdenum nitride: structure, energetics, and vibrational spectra from DFT. Physical Chemistry Chemical Physics. 2014;7.
45. Dahl S, Logadottir A, Egeberg RC, Larsen JH, Chorkendorff I, Törnqvist E, et al. Role of Steps in N2 Activation on Ru(0001). Physical Review Letters. 1999;83(9):1814-7.
46. Lloyd L. INDUSTRIAL CATALYSTS. Handbook of Industrial Catalysts: Springer; 2011.
47. Guo X, Du H, Qu F, Li J. Recent progress in electrocatalytic nitrogen reduction. Journal of Materials Chemistry A. 2019;7(8):3531-43.
48. Cong L, Yu Z, Liu F, Huang W. Electrochemical synthesis of ammonia from N2 and H2O using a typical non-noble metal carbon-based catalyst under ambient conditions. Catalysis Science & Technology. 2019;9(5):1208-14.
49. Evans CD, Kondrat SA, Smith PJ, Manning TD, Miedziak PJ, Brett GL, et al. The preparation of large surface area lanthanum based perovskite supports for AuPt nanoparticles: tuning the glycerol oxidation reaction pathway by switching the perovskite B site. Faraday Discuss. 2016;188:427-50.
50. Li F-F, Licht S. Advances in Understanding the Mechanism and Improved Stability of the Synthesis of Ammonia from Air and Water in Hydroxide Suspensions of Nanoscale Fe2O3. Inorganic Chemistry. 2014;53(19):10042-4.
51. Licht S, Cui B, Wang B, Li F-F, Lau J, Liu S. Ammonia synthesis by N2 and steam electrolysis in molten hydroxide suspensions of nanoscale Fe2O3. 2014;345(6197):637-40.
52. Rod TH, Logadottir A, Nørskov JK. Ammonia synthesis at low temperatures. The Journal of Chemical Physics. 2000;112(12):5343-7.
53. Singh AR, Rohr BA, Schwalbe JA, Cargnello M, Chan K, Jaramillo TF, et al. Electrochemical Ammonia Synthesis—The Selectivity Challenge. ACS Catalysis. 2016;7(1):706-9.
54. Lee HK, Koh CSL, Lee YH, Liu C, Phang IY, Han X, et al. Favoring the unfavored: Selective electrochemical nitrogen fixation using a reticular chemistry approach. Science Advances. 2018;4.

55. Bao D, Zhang Q, Meng F-L, Zhong H-X, Shi M-M, Zhang Y, et al. Electrochemical Reduction of N2 under Ambient Conditions for Artificial N2 Fixation and Renewable Energy Storage Using N2/NH3 Cycle. Advanced Materials. 2017;29.
56. Nazemia M, Panikkanvalappila SR, El-Sayed MA. Enhancing the rate of electrochemical nitrogen reduction reaction for ammonia synthesis under ambient conditions using hollow gold nanocages. Nano Energy 2018;49:316–23.
57. Guo C, Ran J, Vasileff A, Qiao S-Z. Rational design of electrocatalysts and photo(electro)catalysts for nitrogen reduction to ammonia (NH3) under ambient conditions. Energy & Environmental Science. 2018;11(1):45-56.
58. Mathey F. General Topics. Transition Metal Organometallic Chemistry: Springer; 2013. p. 1-24.
59. Schrauzer GN, Guth TD. Photolysis of Water and Photoreduction of Nitrogen on Titanium Dioxide. Journal of the American Chemical Society. 1977;99(22):7189-93.
60. Liu Q, Zhang X, Zhang B, Luo Y, Cui G, CXie F, et al. Ambient N2 fixation to NH3 electrocatalyzed by a spinel Fe3O4 nanorod. Nanoscale. 2018;10.
61. Bhalla AS, Guo R, Roy R. The perovskite structure—a review of its role in ceramic science and technology. Materials Research Innovations. 2016;4(1):3-26.
62. Tejuca LG, Fierro JLG. Structure and Reactivity of Perovskite-Type Oxides. Advances in Catalysis. 1989;36.
63. Sun X, Jiang D, Zhang L, Sun S, Wang W. Enhanced Nitrogen Photofixation over LaFeO3 via Acid Treatment. ACS Sustainable Chemistry & Engineering. 2017;5(11):9965-71.
64. Levy M. Crystal Structure and Defect Properties in Ceramic Materials, Chapter 3: Perovskite Perfect Lattice 2005.
65. Fierro JLG. Structure and Composition of Perovskite Surface in Relation to Adsorption and Catalytic Properties. Catalysis Today. 1990;8:153-74.
66. Shi M-M, Bao D, Wulan B-R, Li Y-H, Zhang Y-F, Yan J-M, et al. Au Sub-Nanoclusters on TiO2 toward Highly Efficient and Selective Electrocatalyst for N2 Conversion to NH3 at Ambient Conditions. 2017;29(17):1606550.
67. Merino NA, Barbero BP, Eloy P, Cadús LE. La1–xCaxCoO3 perovskite-type oxides: Identification of the surface oxygen species by XPS. Applied Surface Science. 2006;253(3):1489-93.
68. Minh NQ, Takahashi T. Interconnect. Science and Technology of Ceramic Fuel Cells: Elsevier; 1995.
69. Song ST, Pan HY, Wang Z, Yang B. Synthesis, Properties and Application of High Conductive LaCr03-Based Ceramic Materials. CERAMICS INTERNATIONAL. 1984;10(4).
70. Yoon JW, Chang H, Lee S-J, Hwang YK, Hong D-Y, Lee S-K, et al. Selective nitrogen capture by porous hybrid materials containing accessible transition metal ion sites. Nature Materials. 2016;16:526.
71. Tezuka K, Hinatsu Y. Magnetic and Neutron Diffraction Study on Perovskites La12x SrxCrO3. JOURNAL OF SOLID STATE CHEMISTRY. 1998;141:404-10.

72. Neumeier JJ, Terashita H. Magnetic, thermal, and electrical properties ofLa1−xCaxCrO3(0⩽x⩽0.5). Physical Review B. 2004;70(21).
73. YU S-H. Hydrothermal/Solvothermal Processing of Advanced Ceramic Materials. Journal of the Ceramic Society of Japan. 2001;109(5):65-75.
74. Cushing BL, Kolesnichenko VL, O'Connor CJ. Recent Advances in the Liquid-Phase Syntheses of Inorganic Nanoparticles. Chemical Reviews. 2004;104(9):3893-946.
75. Haron W, Wisitsoraat A, Wongnawa S. Comparison of Nanocrystalline LaMO3 (M = Co, Al) Perovskite Oxide Prepared by Co-Precipitation Method. International Journal of Chemical Engineering and Applications. 2014;5.
76. Bilger S, Blaf3 G, FOrthmann R. Sol-Gel Synthesis of Lanthanum Chromite Powder. Journal of the European Ceramic Society. 1996;17.
77. da Silva ALA, da Conceição L, Rocco AM, Souza MMVM. Synthesis of Sr-doped LaMnO3 and LaCrO3 powders by combustion method: structural characterization and thermodynamic evaluation. Cerâmica. 2012;58:521-8.
78. Wang S, Huang K, Hou C, Yuan L, Wu X, Lu D. Low temperature hydrothermal synthesis, structure and magnetic properties of RECrO3 (RE = La, Pr, Nd, Sm). Dalton Trans. 2015;44(39):17201-8.
79. Zheng W, Pang W, Meng G, D. P. Hydrothermal Synthesis and Characterization of LaCrO3. Journal of materials chemistry. 1999;9:2833-6.
80. Huang K, Yuan L, Feng S. Crystal facet tailoring arts in perovskite oxides. Inorganic Chemistry Frontiers. 2015;2(11):965-81.
81. Rivas-Vázquez LP, Rendón-Angeles JC, Rodríguez-Galicia JL, Gutiérrez-Chavarria CA, Zhu KJ, Yanagisawa K. Preparation of calcium doped LaCrO3 fine powders by hydrothermal method and its sintering. Journal of the European Ceramic Society. 2006;26(1-2):81-8.
82. Zhang J, Zhang H, Wu J, Zhang J. Electrochemical Half-Cells for Evaluating PEM Fuel Cell Catalysts and Catalyst Layers. Pem Fuel Cell Testing and Diagnosis2013. p. 337-61.
83. Harvey D. Overview of Spectroscopy https://chem.libretexts.org/Bookshelves/Analytical_Chemistry/Book%3A_Analytical_Chemistry_2.0_(Harvey)/10_Spectroscopic_Methods/10.1%3A_Overview_of_Spectroscopy: LibreTexts; 2016 [updated April 24, 2019.April 27, 2019]
84. Bolleter WT, Bushman CJ, Tidwell PW. Spectrophotometric Determination of Ammonia as Indophenol. Analytical Chemistry. 1961;33:592.
85. Verdouw H, Van Echteld CJA, Dekkers EMJ. Ammonia Determination Based on Indophenol Formation with Sodium Salicylate. Water Research 1977;12:399-402.
86. Cullity BD. Diffration 1: The Direction of Diffracted Beams. Elements of X-Ray Diffration1956.
87. Cullity BD. Properties of X-rays. Elements of X-Ray Diffration1956.
88. Scanning electron microscopy (SEM) https://chem.libretexts.org/Courses/Franklin_and_Marshall_College/Introduction_to_Materials_Characterization_-_CHM_412_Collaborative_Text/Electron_and_Probe_Microscopy/Scanning_electron_microscopy_(SEM): LibreTexts; [updated May 3, 2019.May 7, 2019]
89. Carter CB, Williams DB. Electron Diffraction and Phase Identification. Transmission Electron Microscopy2016. p. 81-102.

90. Williams DB, Carter CB. Diffraction from Crystals. Transmission Electron Microscopy: A Textbook for Materials Science. Boston, MA: Springer US; 2009. p. 257-69.
91. Hofmann S. Qualitative Analysis (Principle and Spectral Interpretation). Auger- and X-Ray Photoelectron Spectroscopy in Materials Science: A User-Oriented Guide. Berlin, Heidelberg: Springer Berlin Heidelberg; 2013. p. 43-76.
92. Ul-Hamid A. Introduction. A Beginners' Guide to Scanning Electron Microscopy2018. p. 1-14.
93. Ul-Hamid A. Characteristics of X-Rays. A Beginners' Guide to Scanning Electron Microscopy2018. p. 233-64.
94. Chen G-F, Cao X, Wu S, Zeng X, Ding L-X, Zhu M. Ammonia Electrosynthesis with High Selectivity under Ambient Conditions via a Li+ Incorporation Strategy. Journal of the American Chemical Society. 2017;139:9771–4.
95. Lefrou C, Fabry P, Poignet J-C. Thermodynamic Features. Electrochemistry - The Basics, with Examples: Springer; 2012.
96. Lefrou C, Fabry P, Poignet J-C. Simplified description of electrochemical systems. Electrochemistry - The Basics, with Examples: Springer; 2012. p. 68-70.
97. B. Xu ZL, W. Qiu, Q. Liu, X. Sun, G. Cui, Y. Wu, X. Xiong. La2O3 nanoplate: An efficient electrocatalyst for artificial N2 fixation to NH3 with excellent selectivity at ambient condition. Electrochimica Acta. 2019;298:106-11.
98. Zhang Y, Qiu W, Ma Y, Luo Y, Tian Z, Cui G, et al. High-Performance Electrohydrogenation of N2 to NH3 Catalyzed by Multishelled Hollow Cr2O3 Microspheres under Ambient Conditions. ACS Catalysis. 2018;8(9):8540-4.
99. Han J, Ji X, Ren X, Cui G, Li L, Xie F, et al. MoO3 nanosheets for efficient electrocatalytic N2 fixation to NH3. Journal of Materials Chemistry A. 2018;6(27):12974-7.
100. Celorrio V, Dann E, Calvillo L, Morgan DJ, Hall SR, Fermin DJ. Oxygen Reduction at Carbon-Supported Lanthanides: The Role of the B-Site. ChemElectroChem. 2016;3(2):283-91.
101. Fabian FA, Pedra PP, Filho JLS, Duque JGS, Meneses CT. Synthesis and characterization of La(Cr,Fe,Mn)O3 nanoparticles obtained by co-precipitation method. Journal of Magnetism and Magnetic Materials. 2015;379:80-3.
102. Kallarackel TJ, Gupta S, Singh P, Vander T. Thermodynamic Properties of LaCrO4, La2CrO6, and La2Cr3O12, and Subsolidus Phase Relations in the System Lanthanum-Chromium-Oxygen. Journal of the American Ceramic Society. 2013;96(12):3933-8.
103. Gómez-Cuaspud JA, Perez CA, Schmal M. Nanostructured La0.8Sr0.2Fe0.8Cr0.2O3 Perovskite for the Steam Methane Reforming. Catalysis Letters. 2016;146(12):2504-15.
104. Coşkun M, Polat Ö, Coşkun FM, Durmuş Z, Çağlar M, Türüt A. The electrical modulus and other dielectric properties by the impedance spectroscopy of LaCrO3 and LaCr0.90Ir0.10O3 perovskites. RSC Advances. 2018;8(9):4634-48.
105. Liu H, Du X, Xing X, Wang G, Qiao SZ. Highly ordered mesoporous Cr2O3 materials with enhanced performance for gas sensors and lithium ion batteries. Chem Commun (Camb). 2012;48(6):865-7.

106. Fleisch TH, Hicks RF, Bell AT. An XPS study of metal-support interactions on PdSiO2 and PdLa2O3. Journal of Catalysis. 1984;87:398-413.
107. Moulder JF, Stickle WF, Sobol PE, Bomben KD. Handbook of X-Ray Photoelectron Spectroscopy1992.
108. Fierro JLG, Tejuca LG. Non-stoichiometric Surface Behaviour of LaMO3 Oxides as Evidenced by XPS. Applied Surface Science. 1986;27:453-7.
109. Wu Q-H, Liu M, Jaegermann W. X-ray photoelectron spectroscopy of La0.5Sr0.5MnO3. Materials Letters. 2005;59:1980– 3.
110. Yousaf AB, Imran M, Farooq M, Kasak P. Interfacial Phenomenon and Nanostructural Enhancements in Palladium Loaded Lanthanum Hydroxide Nanorods for Heterogeneous Catalytic Applications. Sci Rep. 2018;8(1):4354.
111. X. Li LL, X. Ren, D. Wu, Y. Zhang, H. Ma, X. Sun, B. Du, Q. Wei, B. Li Enabling Electrocatalytic N2 Reduction to NH3 by Y2O3 Nanosheet under Ambient Conditions. Industrial & Engineering Chemistry Research. 2018;57:16622-7.
112. J. Kong AL, C. Yoon, J.H. Jang, H.C. Ham, J. Han, S. Nam, D. Kim, Y-E. Sung, J. Choi, H.S. Park. Electrochemical Synthesis of NH3 at Low Temperature and Atmospheric Pressure Using a γ-Fe2O3 Catalyst. ACS Sustainable Chemistry & Engineering. 2017;5:10986-95.
113. R. Zhang JH, B. Zheng, X. Shi, A.M. Asiri, X. Sun. Metal–organic framework-derived shuttle-like V2O3/C for electrocatalytic N2 reduction under ambient conditions. Inorganic Chemistry Frontiers. 2019;6:391-5.
114. Zhang X, Liu Q, Shi X, Asiri AM, Luo Y, Sun X, et al. TiO2 nanoparticles–reduced graphene oxide hybrid: an efficient and durable electrocatalyst toward artificial N2 fixation to NH3 under ambient conditions. Journal of Materials Chemistry A. 2018;6(36):17303-6.

Appendix A

Comparison Table of Other Electrocatalysts

A comparison table of other experimental research result of electrocatalysts for NRR is presented in Table A. 1.

Table A. 1: Comparison of the electrocatalytic N2 reduction performance for $LaCrO_3$ with other aqueous-based NRR electrocatalysts

Catalyst	Electrolyte	T	NH_3 yield	FE/%	Ref.
$LaCrO_3$	**0.1 M Na_2SO_4**	**25 °C**	**18.5 μg h^{-1} mg^{-1}_{cat}**	**7.4**	**This work**
La_2O_3	0.1 M Na_2SO_4	25°C	17.04 μg h^{-1} mg^{-1}_{cat}	4.76	(97)
Cr_2O_3	0.1 M Na_2SO_4	25 °C	25.3 μg h^{-1} mg^{-1}_{cat}	6.78	(98)
Y_2O_3	0.1 M Na_2SO_4	25 °C	1.06×10^{-10} mol s^{-1} cm^{-2}	2.53	(111)
γ-Fe_2O_3	0.1 M KOH	25 °C	0.212 μg h^{-1} mg^{-1}_{cat}	1.9	(112)
V_2O_3/C	0.1 M Na_2SO_4	25 °C	12.3 μg h^{-1} mg^{-1}_{cat}	7.28	(113)
TiO_2–rG	0.1 M Na_2SO_4	25 °C	15.13 μg h^{-1} mg^{-1}_{cat}	3.3	(114)
MoO_3	0.1MHCl	25 °C	29.43 μg h^{-1} mg^{-1}_{cat}	1.9.	(99)
Mo	0.01 M H_2SO_4	25 °C	3.09×10^{-11} mol s^{-1} cm^{-2}	0.72	(40)
Au	0.1 M KOH	25 °C	6.042 μg h^{-1} $mg^{-1}_{cat.}$	4.00	(56)

Further results

The results not presented within the report are displayed in this appendix. With Figure B.1 and B.2 showing additional TEM and elemental mapping pictures of the particles. Figure B.3-B.5 showing HRTEM pictures of different parts of the particles. And B.6 showing additional SEM pictures.

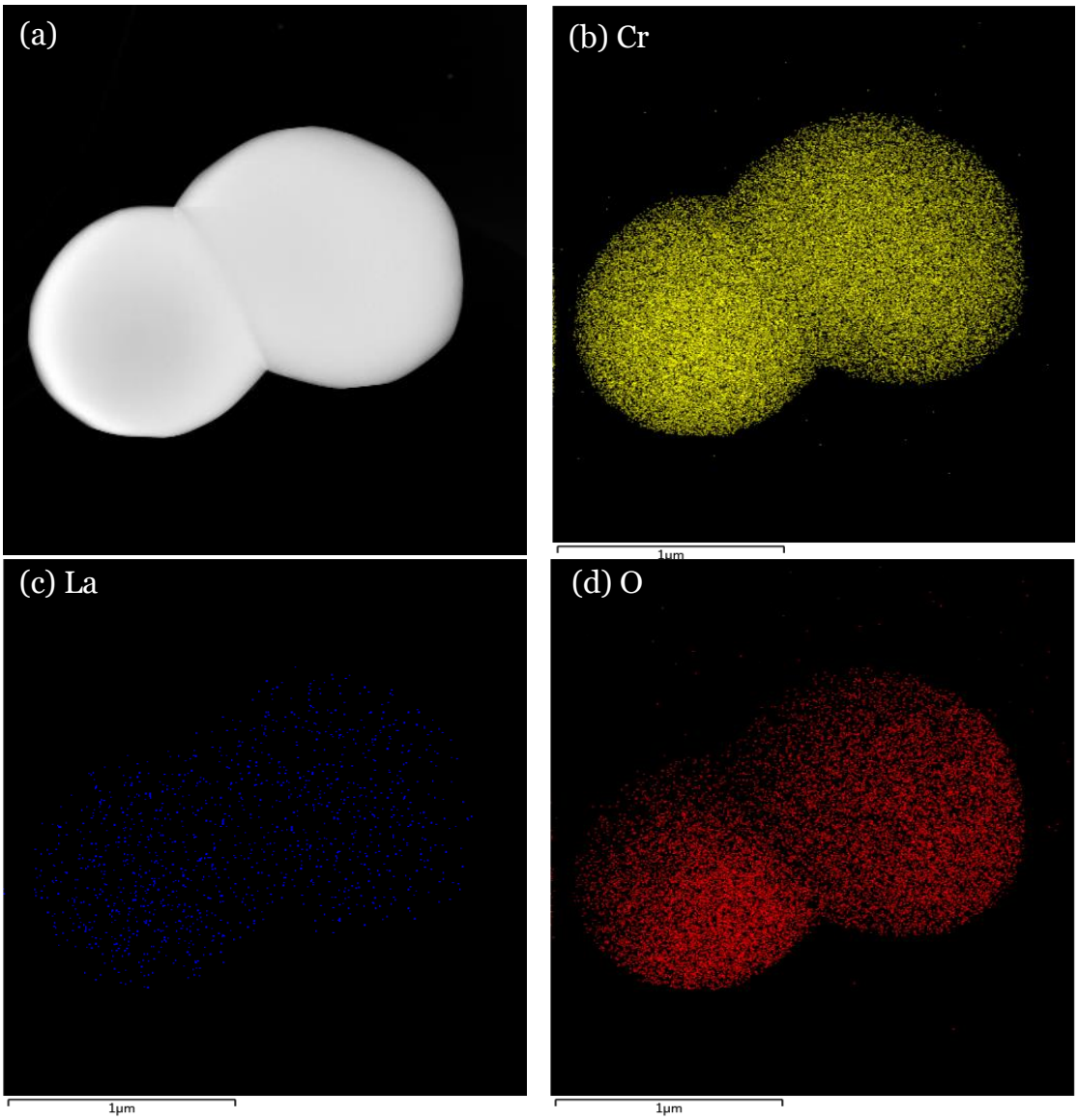

Figure B. 1: TEM image and elemental mappings of La, Cr and O for LaCrO3, showing two particles agglomerated.

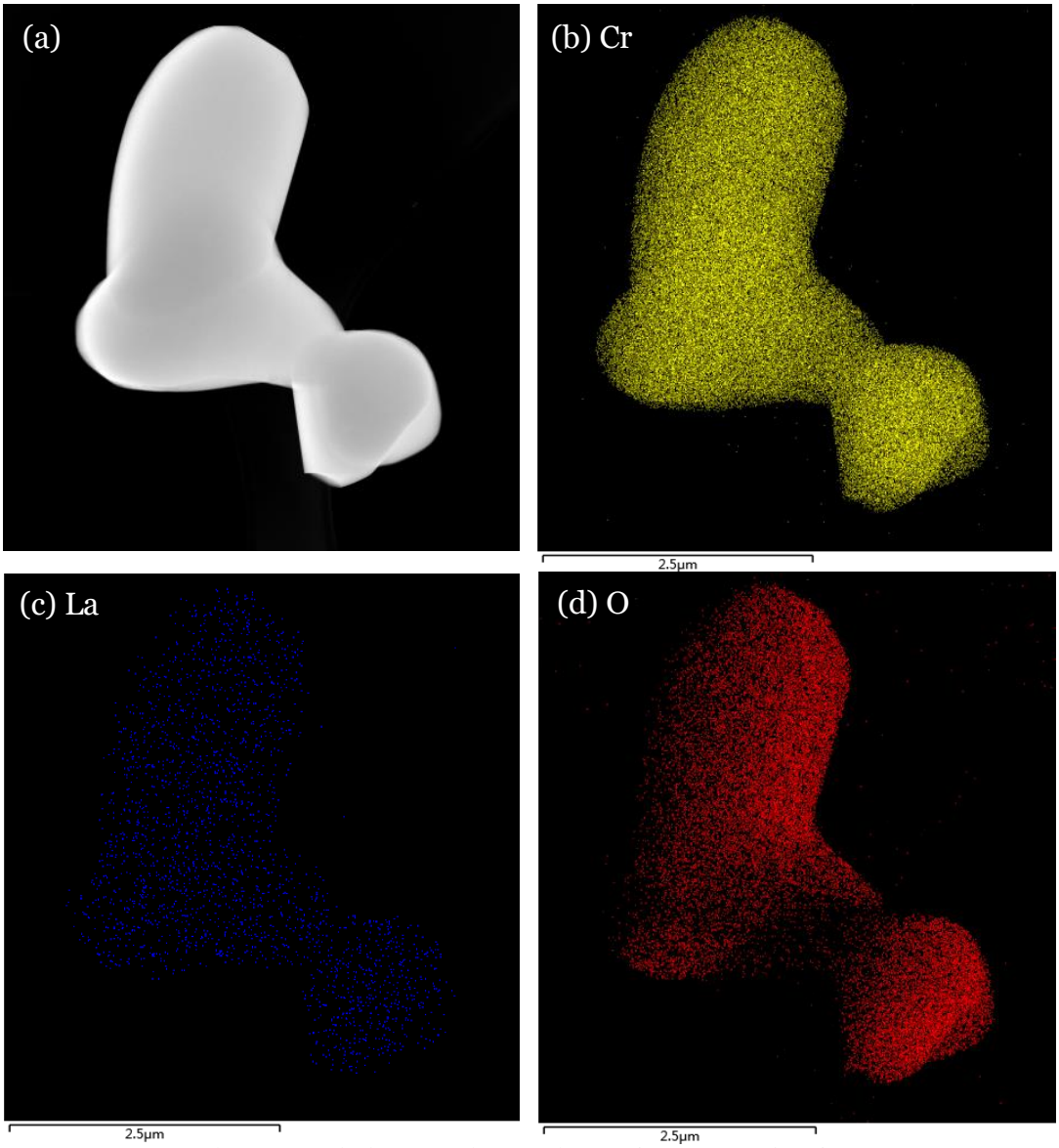

Figure B. 2: TEM image and elemental mappings of La, Cr and O for LaCrO3 agglomerated particles

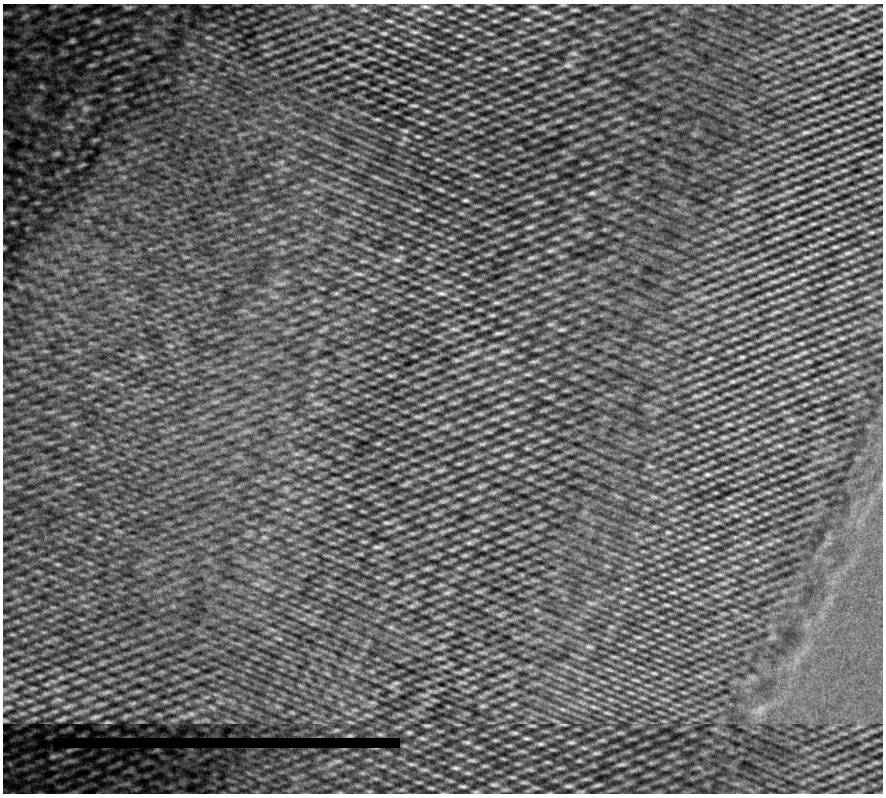

Figure B. 3: HRTEM image of a single $LaCrO_3$ crystal

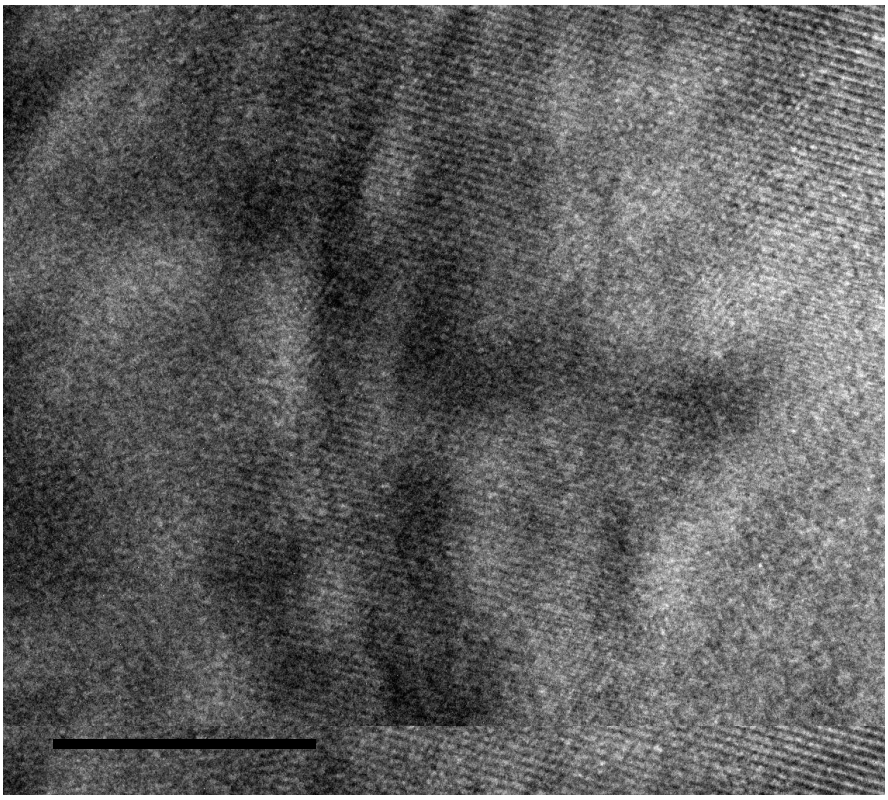

Figure B. 4: HRTEM image of a thicker area of the $LaCrO_3$ particle

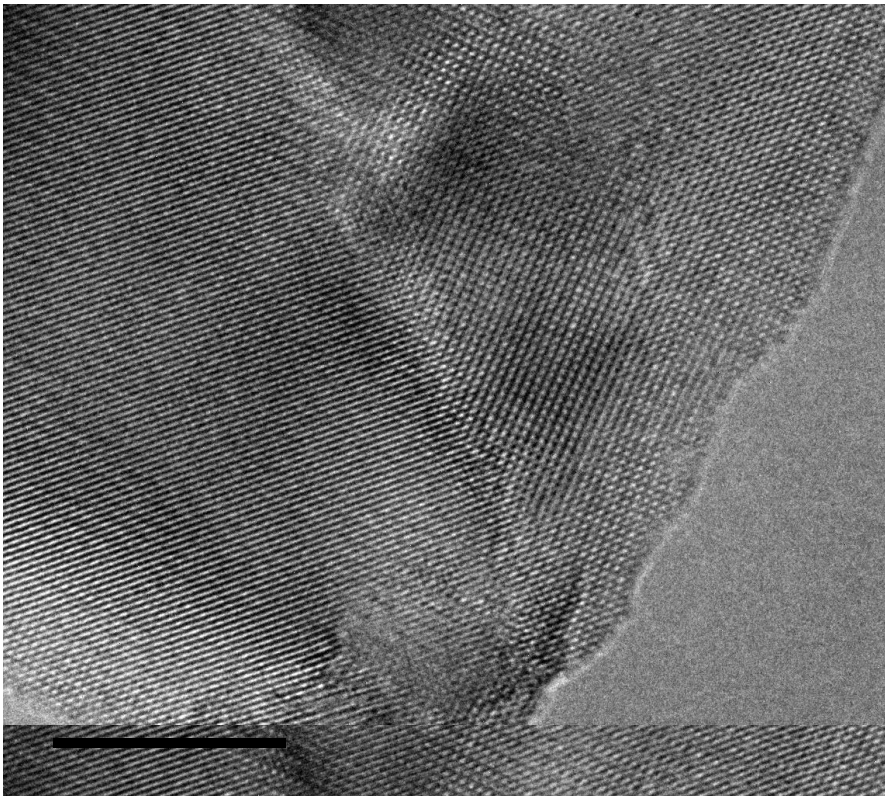

Figure B. 5: HRTEM image of $LaCrO_3$ particle showing a two crystals interaction

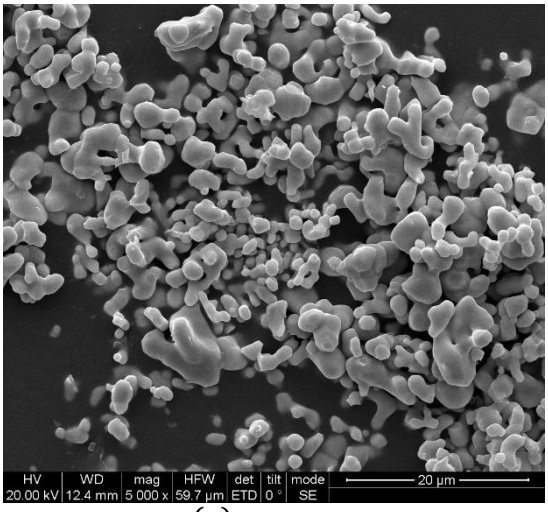

(a) 5000 x

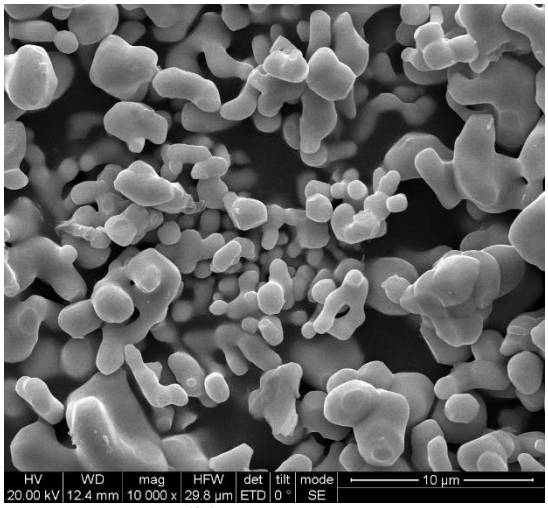

(b) 10 000 x

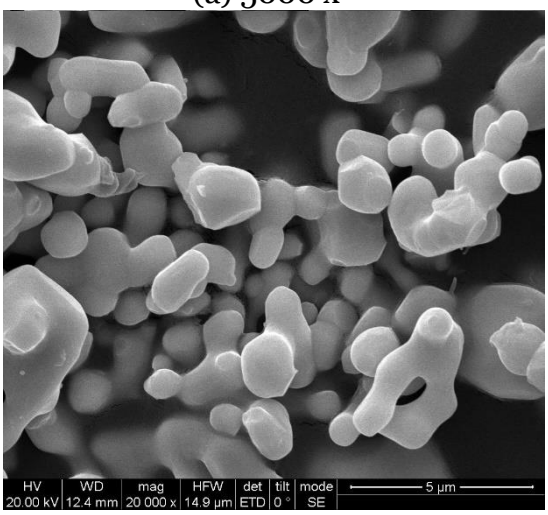

(c) 20 000 x

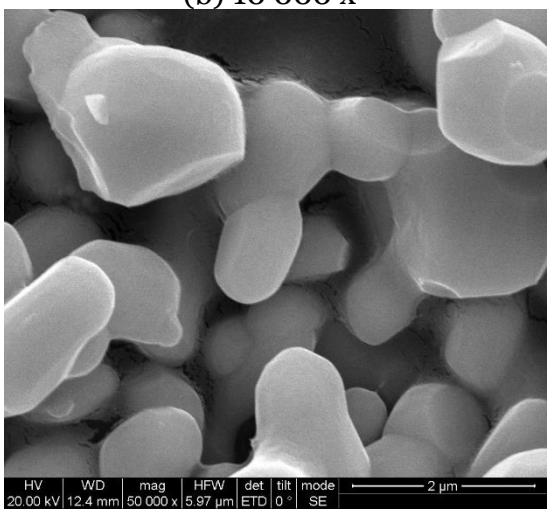

(d) 50 000 x

Figure B. 6: SEM photograph of $LaCrO_3$, second view